Deanship of Graduate Studies

AL- Quds University

Determination of the Pinning Forces and the Scaling Laws Behavior in Al-doped YBCO Superconducting Thin Films near Transition Temperature

Mahmoud Hussein Soliman

M. Sc. Thesis

2002

بسم الله الرحمن الرحيم

Determination of the Pinning Forces and the Scaling Laws Behavior in Al-doped YBCO Superconducting Thin Films near Transition Temperature

By

Mahmoud H. Soliman

(B.Sc.Physics, BierZeit University)

Supervisered by:

Dr. Abdelkarim M. Saleh, Ph.D.

Dr. Mohammed M. Abu-Samreh, Ph.D.

"Thesis Submitted to the College of Sience and Technology at AL-Quds University in Partial Fulfillment of the Requirements for the Degree of Master of Science in Physics".

Abu-Deis, Jerusalem

Palestine

Septemper, 2002

Physics Master/Physics Department
Deanship of Graduate Studies

Determination of the Pinning Forces and the Scaling Laws Behavior in Al-doped YBCO Superconducting Thin Films near Transition Temperature

By:

Student Name: Mahmoud Hussein Ali Soliman

Registration NO.: 9810612

Supervisor: Dr. A. M. Saleh

Co-Supervisor: Dr. M. M. Abu-Samreh

Thesis submitted for examenation on Sunday September 15, 2002 and accepted by the examination committee formed of the following members:

Committee Members		***Signature***
1. Dr. Abdelkarim Saleh	(Committee Chairman)	----------
2. Dr. M. M. Abu-Samreh	(Internal Examiner)	----------
3. Dr. Rushdi Kitaneh	(Internal Examiner)	----------
4. Dr. Hisham Hidmi	(External Examiner)	----------

AL-Quds University

2002

Declaration

I certify that this thesis submitted for the degree of Master of physics is the result of my own research, except where otherwise acknowledged, and that this thesis (or any part of the same) has not been submitted for a higher degree to any other university or institute.

Signed: Mahmoud

(Mahmoud Soliman)

Date: 30.12.2002

Dedication

I would like to dedicate this thesis to my parents, and my wife. I am deeply grateful for their support and help in achieving my graduate study.

Aknowledgments

I would like to express my profound gratitude to my research advisors Dr. Abdelkarim Saleh and Dr. Mohammed Abu-Samreh for their guidance and continuos support through all stages of this work. My thanks will be extended to the faculty and staff members of the physics department for their help and support during my graduate work.

Special thanks to Prof. C. E. Gough group at Brimningham University, UK, for providing us with the magnetization data used in this work.

TABLE OF CONTENTS

List of Illustrations

List of Illustrations *-continued*

List of Illustrations *-continued*

Abstract

Magnetization data of Al-doped YBCO laser ablated superconducting thin films were used to calculate critical temperature, critical currents and magnetization of samples having different dopant concentrations. The results were found to be greatly dependent on dopant concentrations. Magnetization curves of samples with no anomalous behavior have been detected.

The magnetization width was used to estimate the critical current density, J_c. The crtical current results were scaled according to the scaling law $J_c(T) = J_o(T)(1-T/T_c)^n$, where n is an exponential parameter whose typical value is of the order ~ 2.3. Besides, results of the pinning force dependence on temperature for the given samples are also scaled according to the following scaling law:

$$F_h = F_{p0}(T)h^p(1-h)^q$$

where h is the reduced applied magnetic field and p and q are parameters having values of the order of 0.70±0.02 and 1.72±0.05, respectively. The pinning force F_p exhibits a peak in the F versus H_{max} curves. This peak was also scaled according to a power law of the form $F_p \alpha H_{max}^n$. The predicted scaling behaviors are in good agreement with the flux-line shear model (FLS) at low-temperatures as well as around the transtion temperature.

Chapter One

Introduction and general considerations

1.1 Introduction

Superconductivity is a state of some materials that was first discovered by Onnes in 1911 during his study of some physical properties of mercury in the low-temperature region when a mercury sample was cooled down to 4 K (Reitz, Frederick, Milford, and Christy, 1993). The main observation indicated that the resistance of the sample falls rapidly by decreasing temperature until it is completely reached zero around 4.2 K. In another investigation to test the results using more sensitive equipment such as persistent current induced in a loop of superconducting wire, Onnes was able to estimate a resistance value of (10^{-12} Ω) for the mercury metal. The general resistance dependence on temperature for mercury wire as observed by Onnes (Reitz *et al.*, 1993) is shown in Figure 1.1.

In a separate investigation to test Onnes results it was found that an induced current of several hundred amperes in a superconducting ring made of lead has shown no change in the current magnitude for a period of almost one year. The investigation results came in favor of Onnes

observations and confirmed the resistance in the superconducting state is indeed zero (Reitz *et al.*, 1993).

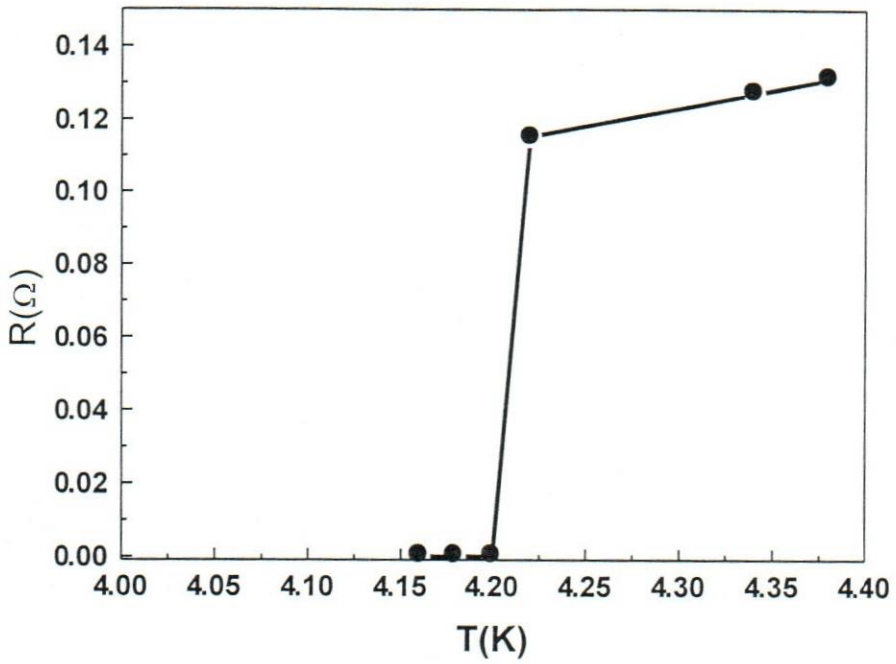

Figure 1.1. Resistance dependence on temperature for mercury.

Shortly after such observations, the superconducting phenomenon had attracted the attention of thousands of scientists during the last century. Investigations were conducted on different metals, copmounds as well as alloys. Early investigations were aimed at exploring physical properties for the so-called low-temperature superconducting materials and alloys and on fabricating such materials. The first attempt for investigating superconducting materials at high transition temperature, T_c, of about 23.2 K was reported in 1973 for Niobium-Germanium thin films

near the stoichiometric composition Nb_3Ge (Tinkham, 1996). More than 20 elements and hundreds of alloys and intermetallic compounds have been prepared and used as superconducting materials.

Since the discovery of superconductors in 1911 until 1986, it was believed that superconductivity is limited to low-temperatures (Robert, and Richard, 1994) ($T_c < 25$ K). In the first half of the year 1986, Bednorz and Muller reported transition temperatures of about 30 K for the, Oxygen-deficient compounds of Barium, Lanthanum, Copper Oxide metallic system (BaLaCuO) (Bednorz and Muller, 1986). After that, the search for a room temperature superconductor began to be intersting. By the end of 1986 other Lanthanum compounds having transtion temperature close to 40 K were fabricated and shortly after that, the Yttrium Barium (YBCO) system superconductor at T_c of about 85-95 K was reported. Early 1988 the superconductivity state has reached a transition temperature of 120 K for both BiSrCaCuO and TiBaCaCuO superconducting systems (Tinkham, 1996). Indeed, understanding the appearance of superconductivity at higher temperatures above 77 K is of major concern in physics today (Robert *et al.*, 1994). In general, every material with transition temperature above 77 K is considered as a member of the high-T_c superconductor (HTSC) family. The temperature dependence of resistance for a typical high-T_c superconductor compound, namely ($YBa_2Cu_3O_7$), is displaced in Figure 1.2.

The discovery of high-T_c superconductors in materials having antiferromagnetic properties opened a new era in physics, technology, and engineering. For the past fifteen years, there has been a dramatic intensification of activity in the superconductor search field at room temperatures (Robert *et al.*, 1994).

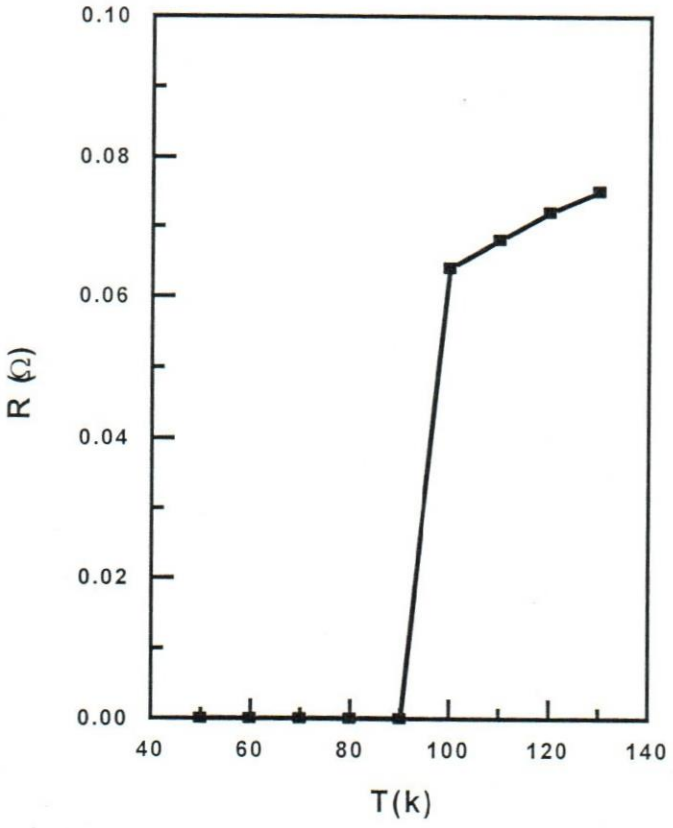

Figure 1.2. Typical resistance dependence on temperature for YBCO high temperature superconductor

All superconducting materials are characterized by several common properties. Firstly, each superconducting metal or alloy is characterized by a transition temperature, T_c. The transition temperature is that temperature at which the state of the metal or alloy transforms

from the normal state to the superconducting state, or equivalently it may be defined as the temperature at which the resistance of the superconductor falls to zero (Rose and Rhoderick, 1978). The transition temperature values for low-temperature superconductors were found to range from about 1 K to about 4 K, while for high-T_c superconductors it might reach as high as 143 K.

Secondly, no magnetic field can be detected inside the superconductor specimen in its superconducting state. This effect was first observed by Meissner during his work to measure the flux distribution outside tin and lead specimens, when cooled below their transition temperature in the presence of a magnetic field (Rose *et al.*, 1978). This experiment has demonstrated that superconductors have additional property that a merely perfect conductor metal would not possess. In general, in its superconducting state a metal never allow magnetic flux to exist in its interior. In other words, a superconductor never has a flux density inside even when a magnetic field is applied. This phenomenon is known as the Meissner effect (Rose *et al.*, 1978) and is illustrated in Figure 1.3. According to Meissner effect, the magnetic induction lines will be ejected as a superconducting sample passes below T_c. Thus inside the superconducting specimen the magnetic field is generally equal to zero ($B_{inside} = 0$) and so the case for the magnetic field flux.

The physical interpretation of Meissner effect is as follows: when a superconductor is cooled in the presence of a magnetic field around its transition temperature, persistent currents are established in the form of circular rings surrounding the metal and resulted in a magnetic flux to cancel the flux intensity inside the superconductor (Ashcroft and Mermin, 1976). Similar argument is applicable when a magnetic field is applied after the superconductor has been cooled.

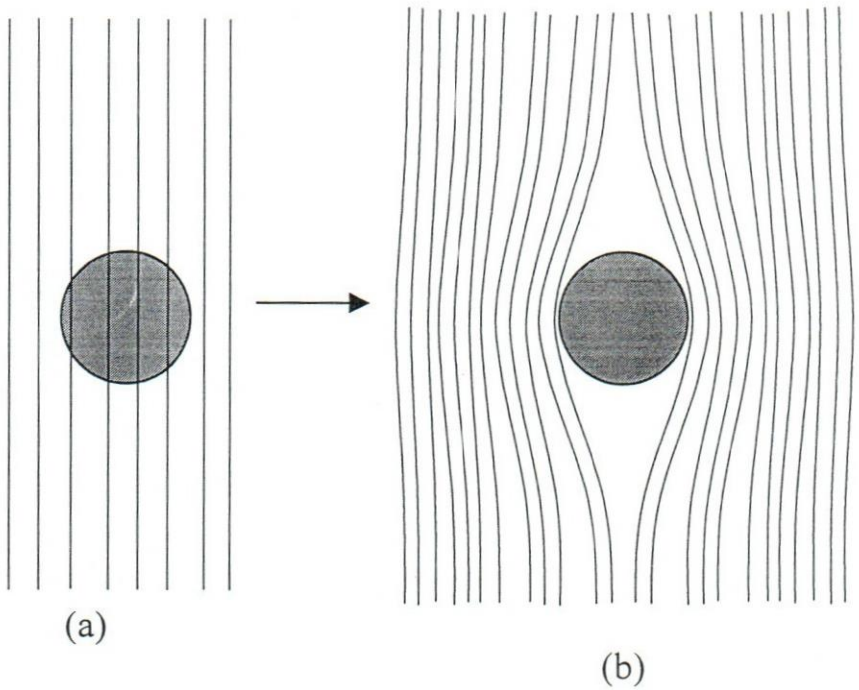

Figure 1.3. Illustration of the Meissner effect in a superconducting sphere when cooled in a constant applied magnetic field. (a) Normal state, (b) Superconducting state.

At the boundaries of the superconductor, the flux intensity decreases rapidly within the region where screening currents exist. The depth within which the current flows is called the penetration depth (λ). The flux of the applied magnetic field is allowed to penetrate the

specimen up to this depth. The penetration depth values are found to vary with temperature and to increase by increasing the metal impurity (James, 1989)

The applied magnetic field has the effect of reducing the transition temperature of a superconductor. The maximum applied magnetic field to a superconductor at a particular temperature while maintaining the superconductivity state of a superconductor is called the critical field, H_c. Therefore, superconducting materials and alloys respond to the applied magnetic field differently, depending on their magnetic behavior. Accordingly, superconductors are generally classified into type-I and type-II superconductors.

The type-I superconductors exhibit a single critical magnetic field level H_c below which zero resistivity, ρ, and zero internal field H_{in} can be established in the presence of an applied external field H_{appl} except in intermediate state conditions. In general, type-I superconductors are pure metals having low critical fields and may be used in the fabrication of some superconducting magnets. Pure metallic samples (such as lead, mercury, and tin) are examples of type-I superconductors (Robert *et al.*, 1994).

It was observed experimentally that under certain conditions, even though the external applied field is less than H_c, some type-I superconducting materials are still having a mixed state of normal and

superconducting states. Those materials remain non-superconducting, because of the coexistence of macroscopic superconducting and normal regions within the specimen. At fields higher than H_c, type-I superconductors revert to the normal state and re-establishes its normal resistance as displayed in Figure 1.4. When external magnetic field (abscissa) is applied to a type-I superconductor, an induced magnetic field (ordinate) is established and cancels the applied field until there is an abrupt change from the superconducting state to the normal state (Figure 1.4).

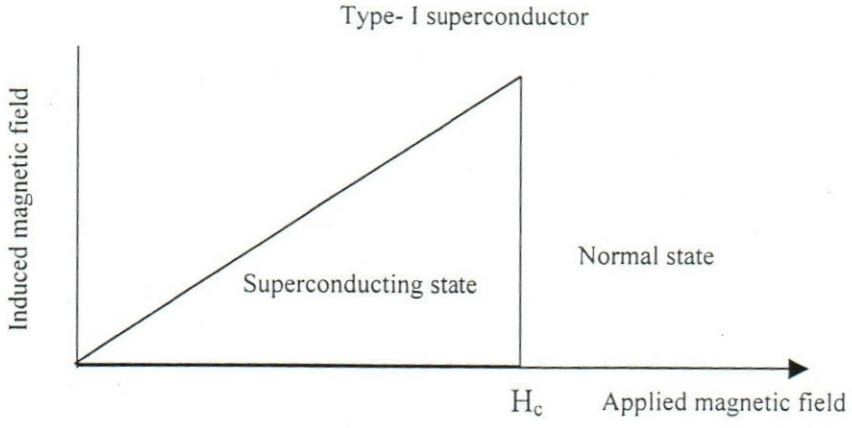

Figure 1.4. Illustration of type-I superconductor behavior in which a perfect diamagnetism is established.

Experimental observations revealed that certain superconductors, especially alloys and impure metals, will not behave quite well as type-I superconductors and an anomalous behavior has been observed frequently. This anomalous behavior is usually ascribed in terms of

impurity effects (Rose and Rhoderick, 1978). Now, it is well understood that anomalous properties of certain superconductors are not merely impurity effects but reveal some natural features of another class of superconductors, the so-called type-II superconductors (Rose *et al.*, 1978). High-T_c ceramic superconductors such as (YBCO) and BiSrCa CuO (BSCCO) are examples of type-II superconductors (Robert *et al.*, 1994).

1.2 The mixed states

1.2.1 The normal and the superconducting states

For all superconductors there are certain superconducting regions within the material at a given temperature and magnetic fields. However, outside these regions the material is normal. Figure 1.5 demonstrates the relationship between temperature and magnetic fields for both the normal state and the superconducting state.

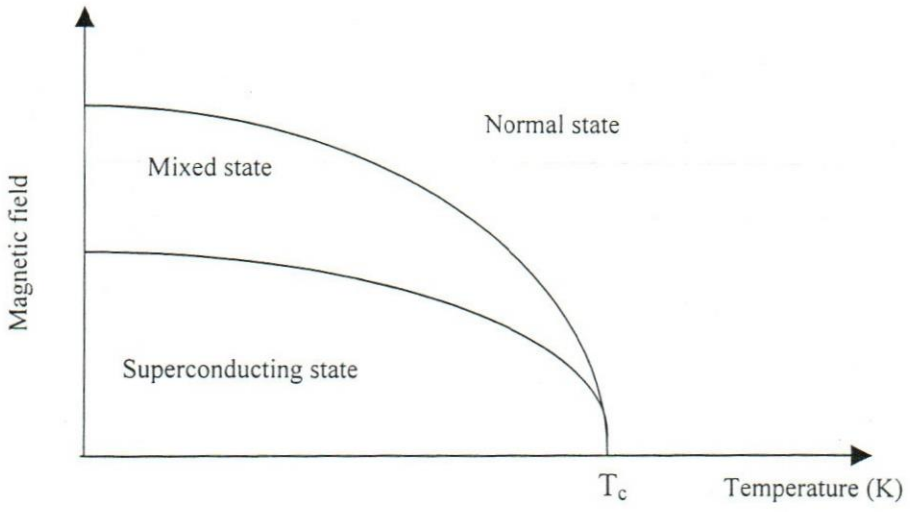

Figure 1.5. A typical magnetic field dependence on temperature showing normal, mixed, and superconducting states in type-II superconductors.

The dependence of the induced magnetic field of type-II superconductor on the applied field is illustrated in Figure 1.6. Clearly, the figure exhibits two critical fields namely H_{c1} and H_{c2}. Below H_{c1} magnetic field lines are excluded from the interior of the superconductor. At field strengths between H_{c1} and H_{c2} the field begins to penetrate into the material. When this penetration happens, the material is said to be in the mixed state (vortex state). In this state, some of the material is in the normal state while the rest is in the superconducting state. In general, type-II superconductors have higher H_{c1} values than those of type-I. The YBCO superconductors have high critical field values about (100 tesla) (Robert *et al.*, 1994).

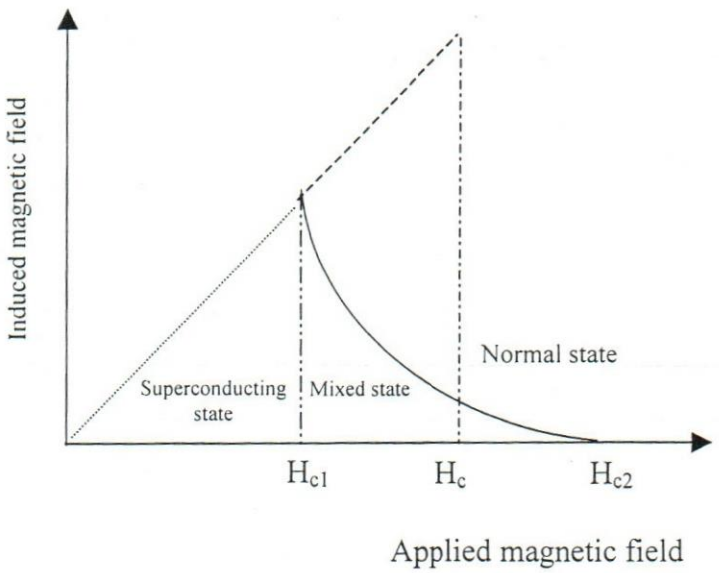

Figure 1.6. Superconducting magnetization of type-II superconductor

The interesting magnetic properties of type-II superconductors help in explaining the Meissner effect. When moving a type-I superconductor magnet, a bowl shape must be used to prevent the magnet from scooting off the superconductor. Some of the field lines of the magnet have penetrated the sample and are trapped in defects and grain boundaries in the crystals. This phenomenon is known as flux pinning. This "locks" the magnetic field to a region above the specimen. The flux pinning produces a field gradient in the superconductor and causes a net current to flow in the material. In the absence of defects, type-II superconductors have no bulk current conducted through the specimen without a transition from the superconducting state into a normal conducting state.

The superconducting state is defined by three important quantities: the critical temperature (T_c), the critical field (H_c), and the critical current density (J_c). Each parameter is dependent on the other two quantities. Maintaining the superconducting state requires that, the magnetic field and the current density, as well as the temperature should remain below the critical values. The phase diagram in Figure 1.7 displays the relationship between T_c, H_c, and J_c. The highest values for H_c and J_c occur at 0 K, while the highest value for T_c occurs when H and J are both zeros. When considering all three parameters simultaneously, the plot represents a critical surface.

When moving from this surface towards the origin, the material is superconducting. Outside this surface, the material regions are all normal or in unstable mixed states. This will lead to a lower energy state for the superconductor and hence electrons can share the same quantum wave function or energy state; in other words they are said to form Cooper pairs. The current density larger than the critical value is forced to flow through normal material. This flow through normal material of the mixed state is connected with motion of the magnetic field lines past pinning sites. For most practical applications, superconductors must be able to carry high currents and withstand high magnetic field without reverting to its normal state.

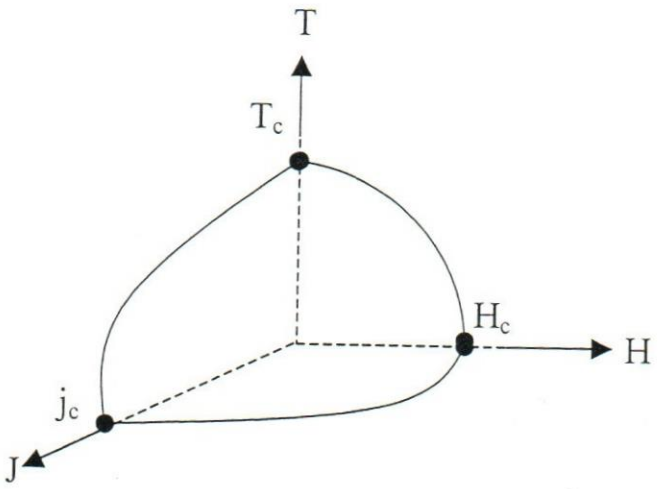

Figure 1.7. Illustration of critical surface diagram

If a type-II material is cooled in a magnetic field, the field lines nomal to the surface are trapped or pinned in the vortex tubes. The stabilization of the pinning sites is important for increasing the value of critical current J_c. Defects play a major role in stabilization of the pinning sites and enhancement of J_c (Kittel, 1996).

Properties of superconducting materials are altered locally by the presence of defects in the materials. A fluxoid encompassing or adjacent to such a defect in the material faces an energy change and inhabitation of its free motion through the superconductor causing flux pinning. In case of small pinning forces, fluxoids may be broken and they might leave their pinning centers, resulting in a net creep of flux through the superconductor that depends on time. This flux creep will result in an effective voltage across the superconductor. If the current density is low and the magnetic field flux is not so intense, the flux creep becomes insignificant (James, 1989). Consequently induced voltage and effective resistance of the superconductor will essentially become zero. At very high fields and current densities, fluxoids will migrate rapidly, giving rise to a phenomenon called flux flow (Murakami, 1992).

1.2.2 The vortex state

One of the most characteristic features of the type-I superconductors is the Meissner diamagnetic effect. The occurrence of perfect diamagnetism implies the existence of a surface energy at the

boundary between normal and superconducting regions in the superconductor. This surface energy plays an important role in determining the superconductor behavior for both type-I and type-II superconductors.

In order to determine the free energy of a superconductor, we consider a superconducting sample in an applied magnetic field having strength less than the critical value H_c. Within the material there are normal regions that result in changing the free energy of the superconductor. Consequently, there will be two contributions to free energy change: the first contribution is due to the bulk of the normal region; the other contribution is attributed to its surface. In an applied magnetic field of strength H_a, the free energy per unit volume of the normal state is greater than that of the perfectly diamagnetic superconductor state by an amount Δg given by the relation (Murakami, 1992):

$$\Delta g = \frac{1}{2}\mu_0(H_c^2 - H_a^2) \qquad (1.1)$$

where μ_0 is the permeability of free space ($=4\pi\times10^{-7}$ T.m/A).

The surface energy between normal and superconducting states is found to be negative in a certain superconducting samples (Rose et al., 1978). In this case the appearance of normal region would result in reducing the free energy. The increase in the bulk energy is outweighed

by the decrease of its surface energy. Normally, the material is supposed to have the lowest total free energy, a large number of normal regions are expected to be formed in the superconducting material to maintain minimum free energy when a magnetic field is applied. Consequently the material is expected to split into some fine-scaled mixture of superconducting and normal regions having boundaries parallel to the applied magnetic field. Such arrangements will produce maximum boundary area relative to volume of normal material. This state is known to be as a mixed or a vortex state. Typical configuration of this vortex state is the one in which the superconductor is threaded by cylinders of normal material (normal cores) lying in parallel to the applied magnetic field as illustrated in Figure 1.8.

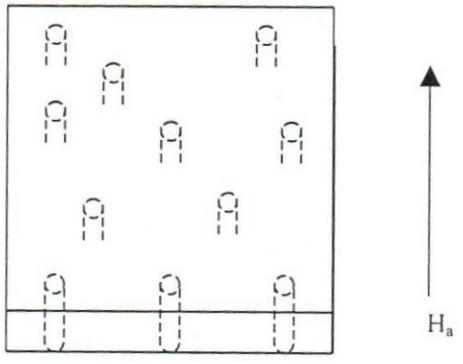

Figure 1.8. Illustration of the vortex state.

Since the bulk of the material is diamagnetic, the flux produced by the applied field will be opposed by a diamagnetic surface current, which circulates around the perimeter of the specimen. Within each core there

will be a magnetic flux directed parallel to the applied magnetic field threading the diamagnetic material. This flux is generated by a vortex persistent current that circulates around the core opposite to that of the diamagnetic surface current. Typical current patterns and the resulting flux are illustrated schematically in Figure 1.9.

The vortex current encircling the normal core interacts with the magnetic field produced by the vortex current encircling any other core. As a result, a mutual interaction will be established between any two cores repeling each other. Because at such mutual interaction, the cores threading a superconductor in the mixed state will arrange themselves into a regular periodic hexagonal array called fluxon lattice.

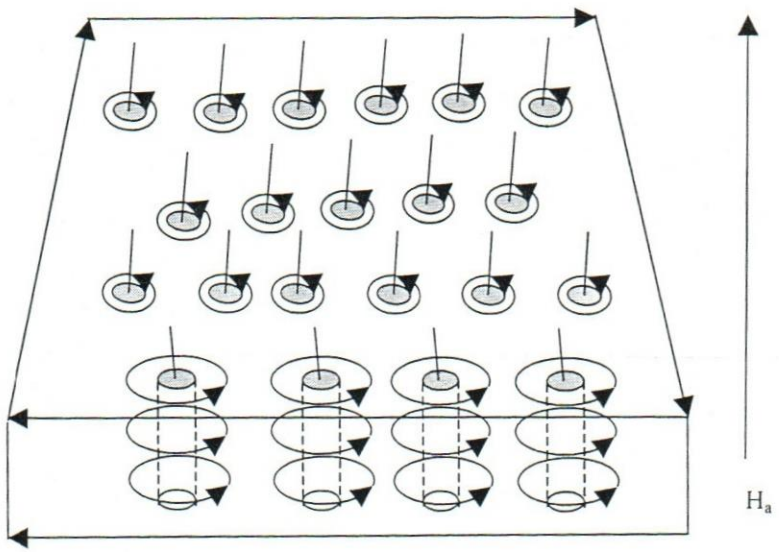

Figure 1.9. Illustration of a taypical vortex state, showing normal cores encircling supercurrent vortices lines that represent the flux threading the cores.

A sharp boundary between superconducting and normal regions cannot coexist in vortex states. The transition is smeared out over a distance, called the coherence length. Besides, the magnetic flux associated with each core spreads into the surrounding into regions a distance equals to the penetration depth (James, 1989).

The superconducting properties vary with position in a periodic fashion when moving towards the center of each vortex. The super-electrons fall to zero. Consequently, along the center of each vortex, there exists a very thin core of normal material as illustrated in Figure 1.10. The dips in the superelectron concentrations are almost two coherence lengths wide apart. The flux density produced by the applied magnetic field will not disappear in the normal cores, but it will decrease to smaller values over a distance of about λ away from the cores. The total flux generated by each core produced by the encircling current vortex is just one fluxon, Φ_o,($\Phi_o = h/2e \approx 2.0678 \times 10^{-15}$ T m^2).

The appearance of a normal core will, therefore, result in a local increase in free energy per unit length of core. This is due to the decrease of electron order. The amount of increase, g_s, in free energy is given by:

$$g_s = \pi \zeta^2 \mu_0 \frac{H_c^2}{2} \qquad (1.2)$$

In a non diamagnetic material and over a radius equals to λ, there will be a local decrease in free energy, g_n, and this decrease is represented by the following expression:

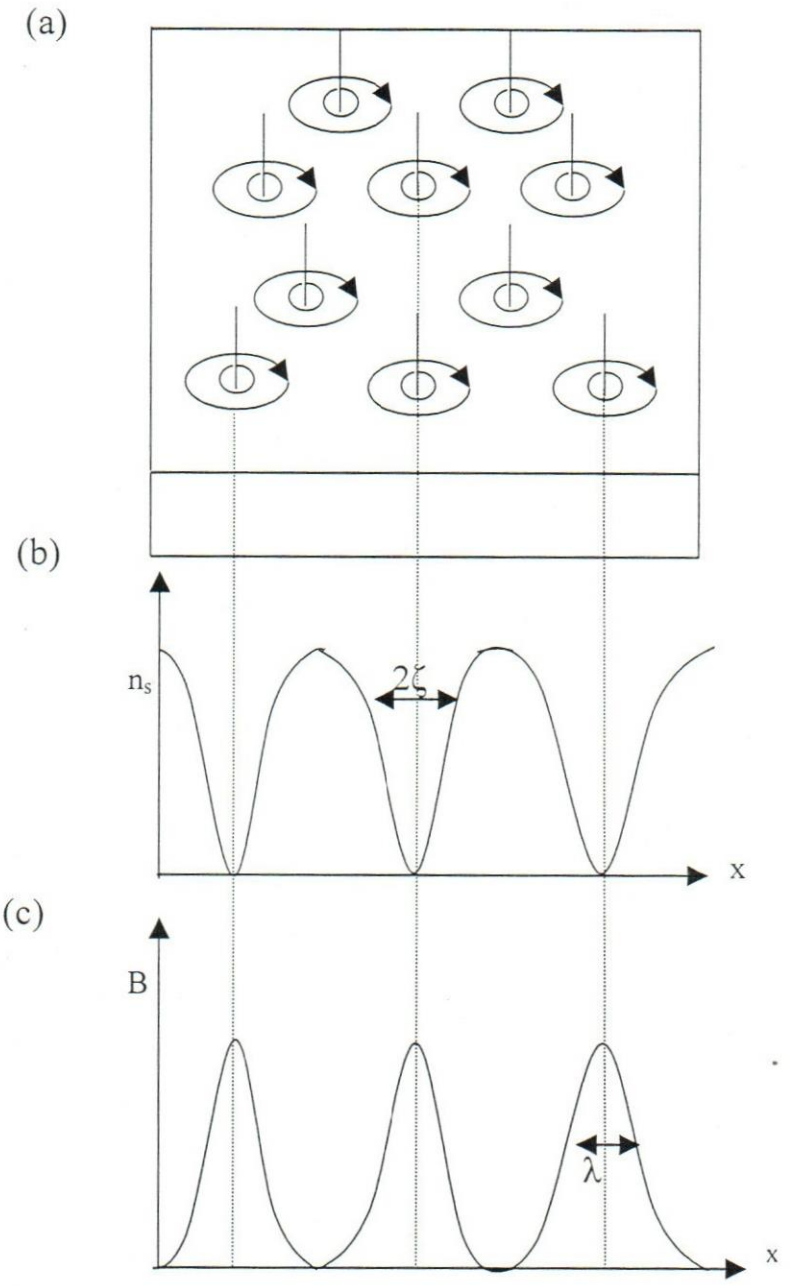

Figure 1.10. A Mixed state in the presence of applied magnetic field of strength just greater than H_{c1}. (a) Lattice of cores and associated vortices, (b) the variation with position of concentration of superelectrons, and (c) the variation of flux density with position.

$$g_n = \pi \lambda^2 \mu_0 \frac{H_a^2}{2} \tag{1.3}$$

When there is a decrease in free energy due to formation of vortex core, the free energy of a superconductivity state is less than that of the normal state, i.e.,

$$g_s < g_n \text{ or } \pi \zeta^2 \mu_0 \frac{H_c^2}{2} < \pi \lambda^2 \mu_0 \frac{H_c^2}{2} \tag{1.4}$$

Accordingly, the appearance of a mixed state in the superconductor is restricted only to coherence length values that are less than the penetration depth or $\zeta < \lambda$.

1.3 The general structure and properties of Yttrium Barium Copper Oxide (YBCO) superconductors

Since this study is aimed at investigating some properties and developing scaling laws of YBCO superconducting thin films, it is of great importance to introduce this material and some of its properties.

The great success obtained with the La-Ba-Cu-O (LBCO) compounds enhanced investigations on other perovskites in the hope that even higher critical temperature superconductors can be produced (Poole Datta, and Franch, 1988). An ultimate goal is to go beyond the 77 K transition temperature value. This would allow the use of liquid nitrogen for operation of the superconductor. The breakthrough was made possible

when the first samples produced were showed resistance transitions above 80 K.

Investigation of $Y_{1.2}Ba_{0.8}Cu_3O_{4-\delta}$ compound characteristics were pioneered by the Wu group (James, 1989). The original sample consists of a mixed phase material, and is known as the 1-2-3 material or the $YBa_2Cu_3O_{7-\delta}$ (YBCO) superconductor, where δ ranges from 0 to ~0.5. The highest critical temperature is associated with the lowest value of δ (James, 1989).

The importance of YBCO superconducting materials is attributed to its doping ability. Not all rare earth elements have been successfully substituted for Yttrium. It should be noted that Yttrium, even though it is typically found with rare earths (in the Minerals Gadolinite, Samarskite, etc.) and has similar properties, it is not considered as rare earth element (Poole *et al.*, 1988). The rare earth elements from Ho to Lu are sometimes referred to as Yttrium earths, because of their resemblance to Yttrium. Apparently, substitution of rare earths for Yttrium may have consequences beyond the scope of theoretical interest (Murakami, 1992).

The chemical structure of YBCO materials has been investigated by means of neutron scattering experiments (James, 1989). The molecular structure of YBCO is illustrated in Figure 1.11. The structure of YBCO may be a tetragonal or an orthorombic depending on the growth conditions:

1-Tetragonal phase (**a**= **b** ≠ **c**)

For this phase δ values vary as $0.6 < \delta < 1$, where the lattice structure is not that of a superconductor, but of a semiconductor. The tetragonal YBCO structure is stable above 650 °C. In this case Yttrium and one copper atom are found in special positions; while the remaining atoms are found in arbitrary positions. Quenching can produce the tetragonal phase at room temperature. The dimensions of the unit cell are a = b = 3.9018 Å, and c = 11.9403 Å.

2- Orthorhombic form (**a** ≠ **b** ≠ **c**)

This is the superconducting phase for $\delta < 0.6$. The representative lattice parameters are as follows: **a** = 3.827Å, **b** = 3.882 Å, and **c** = 11.682 Å. In this form Yttrium atom, one copper atom, and two oxygen atoms are placed in special positions, while the remaining atoms are all in general positions. In this state CuO planes are parallel to the plane of **a b** axes (Poole *et al.*, 1988).

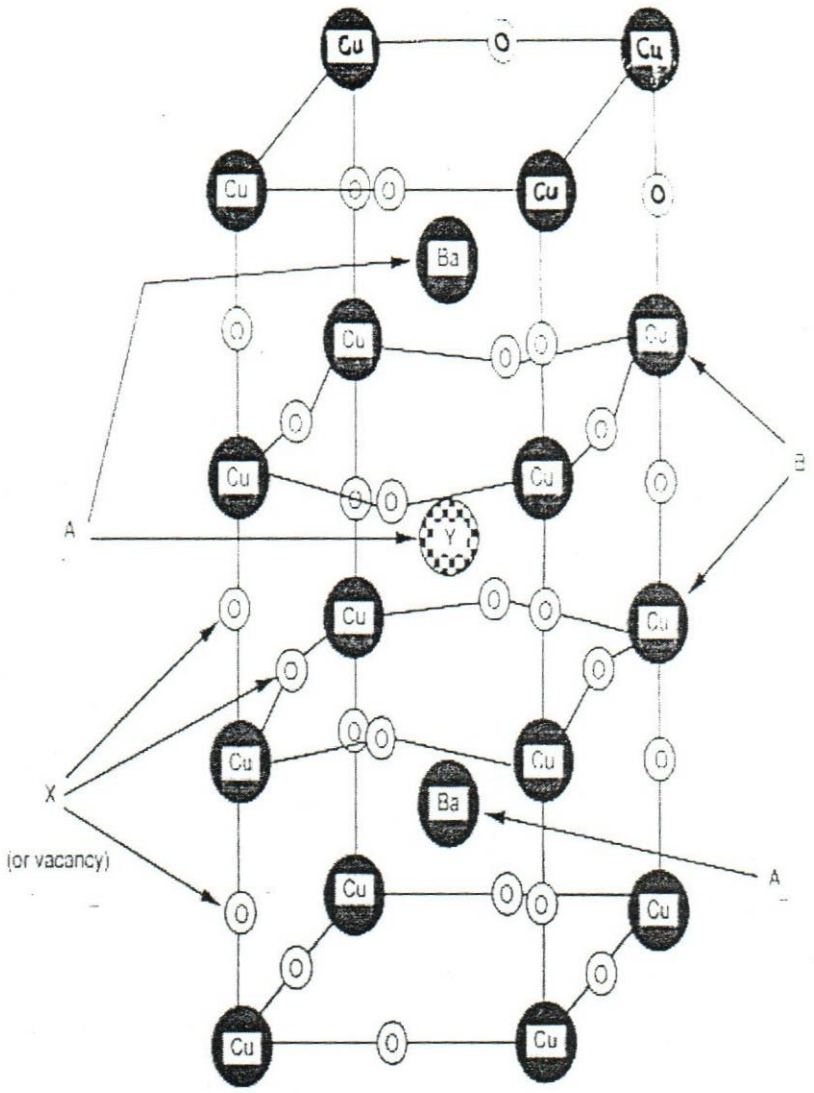

Figure 1.11. Illustration of the 1-2-3 $YBa_2Cu_3O_{7-\delta}$ orthorhombic superconducting structure.

Chapter Two

Theoretical considerations of critical currents, activation energy and scaling laws of high-T_c superconductors

2.1 Introduction

High-T_c superconductors have attracted the interest of many research groups in recent years, because of their importance in many technological applications in general and power applications in particular. For practical applications the critical current density needs to be as high as possible in moderate magnetic fields. Large number of investigators has studied the magnetization and influence of magnetic fields on YBCO (Wen, Rong, Yin, Che, and Zhao, 1995), BSCCO (Zeng Liu, Zhou, Wang, de Boer, and Qiao, 1997), HgBCCO (Abilio, Loureiro, Capponi, and Gorinho, 1995), and many other alloys, in an attempt to understand the magnetic properties of these systems.

This chapter is devoted for discussing some models and their correspondence to critical currents, pinning forces, scaling laws and doping effect on type-II superconductors. The effect of impurities and imperfections that are added or included into the specimen on the critical current values shall be discussed. In addition, the pinning mechanism is described and discussed in some details. Understanding the effect of pinning on the transition temperature, the magnetic field and the critical

current density is of great importance. Besides, understanding scaling laws for the volume pinning force is essential to unify such laws for all superconductors into a single law. Finally, a short brief about the doping type-II superconductors is included.

2.2 The critical currents

The critical current is known as the maximum current that passes through the superconductor specimen, while retaining its zero resistance. If the current exceeds this value, the specimen starts to establish certain resistance. All currents in a superconductor flow at the surface within the penetration depth and the current density decreases rapidly starting from some value, J_a, at the surface. The superconductivity breaks down if the supercurrent density exceeds the critical current density, J_c (Rose *et al.*, 1978).

The charge is transported into and out of the superconducting material by the transport current. When the specimen is placed in an external applied magnetic field, the screening currents circulation will cancel the flux inside the material. At any point J_c, can be considered to be the sum of transport current and screening current components. If the magnitude of the total current density, at any point exceeds J_c, the superconductivity will be broken and the associated magnetic field strength at the surface is that of the critical field strength H_c.

Type-II superconductors are said to be in a complete superconducting state if the field strength is less than H_{c1}. On the other hand, it is said to be in the mixed state when the field strength is greater than H_{c1} and less than Hc_2. The non-zero resistance is a principal characteristic of the mixed state (James, 1989). In case of weak applied magnetic field, the superconductor may not be driven to mixed state, and the critical current can be determined by Silsbee's criterion rule for type-I superconductor (Rose *et al.*, 1978). Accordingly, the critical current is controlled by the perfection of the material. This dependence of the critical current on the perfection of the material is of considerable technical importance because superconductivity electromagnets require zero resistance materials of high current carrying capacity (Murakami, Yamaguchi, Fujimoto, Nakmura, Taguchi, Koshizuka, and Tanaka, 1992).

When a current passes through a type-II superconductor that can be driven into the mixed state by an applied magnetic field, the current flows not only at the surface, as in type-I superconductor, but also throughout the whole body of the material (Rose *et al.*, 1978). The superconducting state is more stable than the normal conducting state at temperatures below the critical temperature. Forming cooper pairs can lower the energy of electronic system of the superconductor. The gained energy

making transition from the normal to superconducting state is known as condensation energy, u, and it is given by

$$u = \frac{1}{2} N(E_f) \Delta^2 \qquad (2.1)$$

where $N(E_f)$ is the density of states at the Fermi energy level and Δ is the energy gap.

The condensation energy is calculated using the thermodynamical critical field, H_c. According to Meissner effect, the superconductor repels the magnetic field completely. Therefore, excess energy in type-II superconductor is needed to expel all magnetic field lines from the specimen and at some critical field. This energy approaches the condensation energy, at critical field H_c. The condensation energy density (condensation energy per unit volume) can be approximated by:

$$u_s - u_n = \int_0^{H_c} B \, dH = \frac{1}{2} \mu_0 H_c^2 \qquad (2.2)$$

where u_s is the energy density of the superconducting phase and u_n is the energy density of the normal phase.

When current passes along the superconductor, the kinetic energy of electrons ($=n_s m v^2/2$, where n_s is the density of the superelectrons) is added to the superconducting state energy. When the kinetic energy is equal to the condensation energy, the superconducting state is no longer

stable and the critical current density, J_c, of the superconductor becomes ideal. In this case, we may write:

$$\frac{1}{2}n_s m v^2 = \frac{1}{2}\mu_0 \lambda^2 J_c^2 = \frac{1}{2}\mu_0 H_c^2 \qquad (2.3)$$

Solving equation (2.3) for J_c, we get

$$J_c = \frac{H_c}{\lambda} \qquad (2.4)$$

The highest values of J_c are set by the deparing current sets for superconductor practical purposes. If its value is lower than the required level, the system cannot be used for practical application. At 77 K, YBCO has H_c of 2.4×10^5A/m and λ of 10^{-7} m, which gives a J_c value of about 2.4×10^{12}A/m^2. This value is three order of magnitudes larger than the required value, indicating that oxide superconductors have intrinsically an increase in J_c values (Murakami, 1992).

2.3 The pinning mechanism

At fields above H_{c1}, type-II superconductor resistance is not quite zero and it is unable to sustain a persistent current unless some mechanism is presented to prevent the Lorentz force from moving vortices. The so-called pinning mechanism has the effect of pinning the

vortex to a fixed location in the material. Pinning is resulted from any spatial inhomogeneity of the material because of local variations of ζ, λ, or H_c due to impurities, grain boundaries, etc. The variation of ζ, λ, and H_c will produce local variations of the free energy per unit length of a flux line. Consequently, some locations of vortices may be favored over others. If the pinning force is sufficiently strong, the vortex motion can be made small enough so that the superconductor may act very much like a perfect conductor. However, for strong currents, there will be a thermally activated flux creep in which vortices hop from one pinning site to another (Tinkham, 1996). In some cases flux creep will occur at a measurable rate. If the steady motion of vortices is limited by viscous drag, then, the regime of flux motion is referred to as flux flow. This kind of motion is usually combined by resistivity flow and is comparable with the resisitivity of the material in the normal state (Tinkham, 1996).

It is well known that the superconducting state has lower energy than the normal conducting state and the magnetic field enters the superconductor to compensate the energy needed to repel the magnetic field when the external field exceeds H_{c1}. The system can lower its energy by allowing the magnetic field to enter the superconductor, although the region where the fluxoid penetrates loses the condensation energy. Therefore, the loss of energy due to the penetration of the fluxoid

is called the penalty energy. The penalty energy per unit volume is given by equation (2.2).

When the fluxoid interacts with non-superconducting region, then penalty energy can be saved as energy per interacting volume. Since such region is in the normal conducting state (Murakami, 1992), then the total saved energy is given by:

$$U_p V = \frac{1}{2}\mu_0 H_c^2 \pi \zeta^2 d \qquad (2.5)$$

where d is the size of the non superconducting region and V is the volume of the non superconducting particle. In other words, the penalty energy must be supplied to move the fluxoid from normal to superconducting region, whereby the fluxoids are pinned at normal regions. It is also clear that the fluxoid can be pinned even by a superconducting region when H_c is small compared to the applied magnetic field. In this case the penalty energy is very small, and the flux pining is less effective than normal regions. The pinning force is generally expressed by the following mathematical formula (Murakami *et al.*, 1992):

$$f_p = \frac{dU}{dx} \qquad (2.6)$$

For a regular cylinder, the pinning force is found to have an expression of the form:

$$f_p = \frac{U}{2\zeta} = \frac{B_c^2}{4\mu_0}\pi\zeta \, d \qquad (2.7)$$

The bulk pinning force, F_p, per unit volume, is obtained from equation (2.7) by summing over all the contributions from various pinning centers. Thus, for N equals the number of interactions per unit volume within the specimen, then the total (bulk) pinning force:

$$F_p = \sum f_{pi} \qquad (2.8)$$

This is the condition for introducing pinning centers to get high J_c in almost all high-T_c superconductors. This implies that pinning centers should be introduced in such a way to achieve large J_c values.

2.4 Scaling laws for the volume pinning force in high-T_c superconductors

In conventional hard type-II superconductors, the general form of the scaling law of the volume pinning force can be written as (Fietz and Webb,1969).

$$\vec{F}_p(B,T) = \vec{B} \times \vec{J}_c(B,T), \qquad [N/m^3] \qquad (2.9)$$

It was found that F_P can also be scaled with a magnetic induction as a single function f(b) where b is the reduced magnetic field ($b=B/B_{max}$) (Fietz, and Webb, 1969), and that the shape of the F_p curve is independent

of temperature. In this model, the force scaling law has the following form:

$$f(b) = b^{1/2}(1-b)^2 \qquad (2.10)$$

The general form of F_p has the following general equation (Dew-Hughes, 1974) :

$$F_p(b,T) = F_{p0}(T)\, b^p (1-b)^q \qquad (2.11)$$

where the exponents p and q depends on the geometry of the defect, the type of interaction and the type of the pinning center.

Another important development is obtained on the basis of the so-called the flux-line lattice (FLL) shear model proposed for conventional superconductors (Kramer, 1973). In an intensive study for developing a scaling law of the pinning forces in normal type-II superconductor, it has shown that this scaling law is given by (Kramer, 1973):

$$F_h = F_{po}(T)\, h^p (1-h)^q \qquad (2.12)$$

where h is the reduced applied magnetic field ($h=H_a/H_c$) and the exponents p and q are parameters that can be adjusted to yield all information about the various involved mechanisms such as thermal activated flux-motion, flux-creep and flux-line lattice shear (Niel, 1992). Such development was tested on artificially structured films (Pruymboom, Kes, Van der Drift, and Radelaar, 1988). All of these

models have been introduced and developed for the description and interpretation of experimental results of the physical properties for a variety of high-T_c superconducting materials.

The presence of scaling laws can give some insight into the flux pinning properties of a material. It was found that in high-T_c superconductor the thermally activated processes play an important role in destroying the scaling behavior of the pinning force (Campbell and Evetts, 1972). Concerning YBCO superconducting thin films, there are several reports on pinning force in undoped YBCO (Pan, Gaponov, Kaminsky, Kuzin, Matsui, Prokhorov, Strikovsky, and Tretiachenko, 1989) doped YBCO (Li, de Boer, Roeland, Kadowaki, Menovsky, Feanse, 1990) and irradiated YBCO (Civale, McElfresh, Marwick, Holtzberg, and Field, 1991). However, scaling is often investigated in a limited temperature range only, and was found not to be perfect in most cases. All reports have shown many different details with some common observations. The scaling field is not H_{c2} but the irreversibility field H*, where the value of J_c drops to zero. In this case, the maximum pinning force is between 0.20 H* and 0.33 H* (Niel, 1992). The downset of pinning force curves is not easy to determine because of the tails at the higher field end. In the region, $H^* < H < H_{c2}$, $J_C \approx 0$, and in the presence of thermally activated flux motion, the pinning force scaling law in its general form could be written as (Niel, 1992).

$$F_p(b,T) = F_{p0}(T)f(b^*) \qquad (2.13)$$

The scaling law given in equation (2.13) includes the necessary conditions for such a pinning mechanism scaling and gives expressions for f(b*) in the framework of different models.

2.5 Doping effects on scaling laws and pinning mechanisms

Introducing the pinning centers, such as metals or non-superconducting particles, to achieve high critical current densities. It was found that there are many elements that can achieve high currents among these silver, copper, iron, cobalt, etc. For instance, the microstructure and the physical properties of YBCO superconducting thin films were improved by silver doping. Films doped by silver have showed four times higher J_c values than the undoped YBCO films (Kalyanaraman, Oktyabrsky, and Narayan, 1995). In general, the critical current increases by increasing the impurity of the superconductor. Moreover, the critical transition temperature is also found to depend strongly on the dopant concentration.

In YBC_{1-x}-M_xO films, (where M is an element like Ni, Al, with x up to 11% dopant concentration) the critical temperature $T_c(x)$ decreases with increasing x for most ceramic samples (Ji, Geng, Chen, Yu, Sun, Chen, Yang, and Jin, 1997). The investigated samples include single crystals, thin films, powders, and bulk material. Valuable information

about the behavior of critical currents (Oussena, De Groot, Marshall, and Abell, 1994), pinning forces (Hermann, Sheng, Kiehl, El-Ali, Hambourger, Almassan, Estrada, and Data 1988), irreversibility lines (Obara, Sawa, and Kosaka, 1994), flux motion and vortex transition (Gupta, Tuset, Kakut, and Fossheim, 1996) were extracted from such investigations (Kung, McHenry, Maley, Kes, Laughlin, and Mullins, 1995). The differences in hysteric response, flux pinning and critical currents are attributed to the various types of interactions between the supercurrent and the intrinsically pinned pancake vortices. This conclusion is drawn from an extensive study of magnetic properties of Bi-based superconductor in the form of single crystals or Ag-sheathes tapes (Krusin-Elbaum, Civale, Vinokur, and Holtzberg, 1992).

Civale (1991) has studied the pinning force F(B,T) in $YBa_2Cu_3O_7$ crystals as a function of flounce of 3 MeV protons. For a given ion-damage level, all F_p data can be reduced to a single function in terms of the reduced field h ($h = H/H^*$), where $H^* << H_{c2}(T)$ is the scaling filed related to the irreversibility line.

Critical current measurements in conventional hard type-II superconductors are usually analyzed in terms of the volume pinning force $F_p(b)$, where $F_p = Bj_c$ and $b = B/B_{c2}$ is the reduced magnetic field. In many cases a scaling law having the form $F_p = F_{po}(T)b^p(1-b)^q$ is examined. This type of scaling provides important information on the

relevant pinning mechanism through the exponents p and q (Niel, 1992). In this case, the influence of thermally activated flux motion on the measured volume pinning force is also included.

At high temperatures F_p is determined not only by the de-pinning critical current $J_{co}(B,T)$ (in the absence of thermal activation), but also by the activation energy U(J,B,T). Therefore, the usual scaling law should be modified to include the activation energy effects (Niel, 1992). It was shown that for low-scaled field (h) region, this behavior can be described qualitatively well on the basis of the extended critical state model. The effective activation energy extracted from magnetic relaxation measurements can also be qualitatively described by a scaling relation that fits with the collective pinning theory (Xiao, 1997).

The flux pinning force density F_p in a series of 3d- transition metal elements (Fe, Co, and Ni) doped Y-Ba-Cu-O thin films has been measured as a function of magnetic field, temperature, and doping concentration (Song, Yang, Chen, and Kao, 1992). Generally, F_p has shown an interesting double-peak behavior separated by the critical field H*. This feature is attributed to the flux-line configuration in thin films placed in a transverse field. A universal scaling law for the pinning force was derived to include all the variations of the pinning force with the field, the temperature, and the doping concentration (Song *et al.*, 1992).

Magnetization measurements have been performed on **c**-axis oriented superlattice films of YBaCuO/ PrBaCuO over a wide range of temperatures (4.2 K - 70 K) and magnetic fields (0-8 T). When the magnetic field is applied parallel to the C-axis, the pinning force scaling can be written as (Shi, Ji, and Yao, 1993):

$$f_p \alpha \ (1-t)^{2.7} h^m (1-h)^n \qquad (2.14)$$

where t is the reduced temperature ($t = T/T_c$), and h is the reduced field. The exponent m ranges from 0.9 - 0.7, while n ranges from 1.8 - 3, depending on the sample thicknesses. This result indicates that flux pinning centers in YBaCuO/PrBaCuO films are strong over a wide range of the field *h*. The dependence of the domelike F_p on the exponents m and n for samples with different thicknesses of the PrBaCuO layer manifests that the dynamical property of the flux-line lattice plays an important role in the volume pinning force density. The derivation of F_p from the scaling law in high reduced field h is obtained on the basis of giant flux creep or collective pinning (Shi *et al.*, 1993).

Chapter Three

Experimental considerations for data measuerments

3.1 Introduction

The magnetization data used in this study were provided by Prof. Gouph's research group at Brimingham University, UK. These data are analyzed in order to determine critical current densities and pinning forces of Al-doped YBCO superconducting thin films and their relating scaling laws are examined in the next chapter.

In this chapter, we shall focus on discussing briefly the experimental procedures used in the preparation of YBCO thin films by means of solid state reaction and laser Excimer co-evaporation method. Some measurements of the magnetization loops will be included and briefly described.

3.2 The sample material preparation

The well-known method for preparing high-T_c samples is the so-called solid state reaction method (Poole, Datta, and Franch, 1988). However, this method has the advantage of being relatively rapid, the additional undesirable phases introduced to the sample during the preparation procedures are considered to be the most disadvantage known of this method (Chen, Sang, Golbeng, Sung, McMichael, Gaincs, 1987). In general, the solid state reactions begin with either the carbonate or

oxide forms of the individual constituents with several stages of grinding and mixing are involved.

In order to obtain highly oriented samples, a melt textured growth process is employed. In this method the sintered YBCO sample is melted and slowly cooled in a thermal gradient. The preferred orientation for grain growth is known as the **a-b** plane along which grains can be aligned (Murakami, 1992).

The pinning centers are generally introduced into the films to obtain higher J_c values by making use of the following two processes, the quench-melt-growth process and the melt- powder-melt growth process (James, 1989).

3.3 Preparation of high-T_c superconducting films using laser co-evaporation

High-T_c thin films of excellent quality are now commonly produced by laser Excimer co-evaporation, that is, multiple laser beams on specific constituents of the superconductor that are to be evaporated onto the substrate (James, 1989). With lasers it is relatively easy to focus on a very small target area such as small pellets are used as the primary source of high-T_c material. Thin films of $YBa_2Cu_3O_x$ material were deposited by illuminating a bulk sample of $YBa_2Cu_3O_{7-\delta}$ with a pulsed Excimer laser (Wu, Ashburn, Trong, Hor, Meng, Gao, Huang, Wang, and Che, 1987). Laser induced evaporation from the pellet is deposited on the

heated substrate. Figure 3.1 displays how pulsed laser Excimer evaporation technique is used to produce thin films from a bulk of Y-Ba-Cu-O pellets.

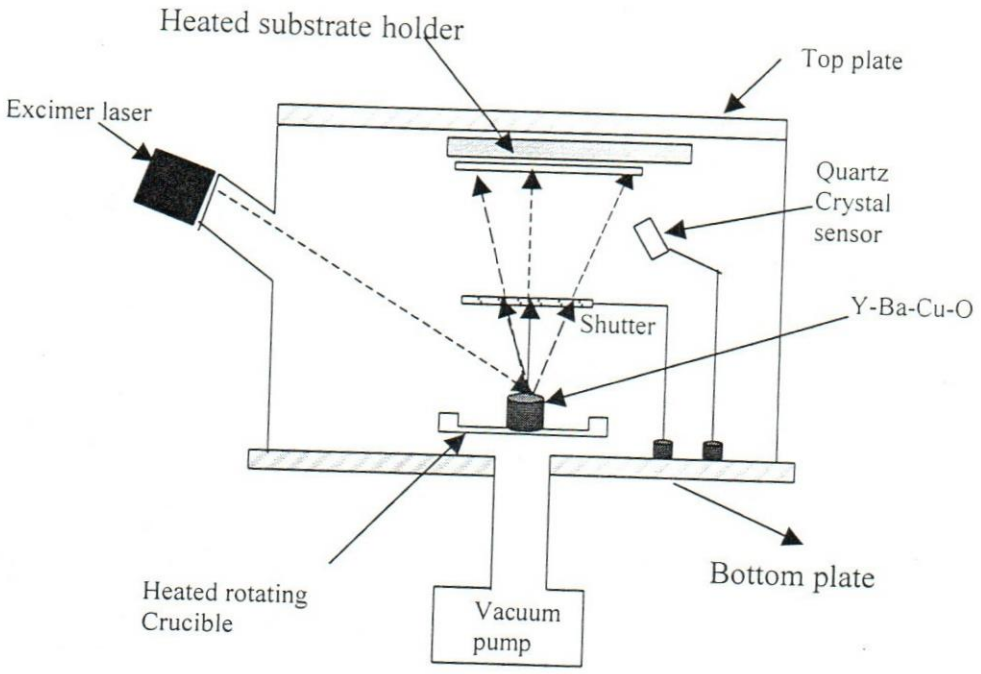

Figure 3.1. Illustration of pulsed laser Excimer evaporation technique.

The method of co-deposition and ex-situ annealing has demonstrated its effectiveness by producing undoped $YBa_2Cu_3O_{7-\delta}$ superconducting thin films with high-T_c and large J_c. Besides, the capability of the technique was extended to include the fabrication of doped $YBa_2 (Cu_{1-x}Al_x)O_{7-\delta}$ films (Kim J-Tae, Xenikos, Thorns, and Lemberger, 1992).

In general, the AL-doped YBCO superconducting thin films were fabricated by pulsed laser ablation from stoichiometric $YB(Cu_{100-x}Al_x)O$ sintered for x = 0 - 5, targets. A 248 nm wavelength Excimer laser with a pulse length of 20 nm and a repetition rate of 10 Hz was employed as the light source (Slaski, Woodall, Wellhofer, Yeadon, and Gourgh, 1996). The estimated laser pulse fluence on the surface of the rotating target was 1.5 J cm^{-2} focused on an area of 2×5 mm^2. Each deposition was performed over a 15 min period in 400 mTorr background pressure of high purity O_2. Upon completion, O_2 was leaked into the chamber to a pressure of 1 atmospheric pressure. The film was allowed to cool to room temperature at 30 $^{\circ}C$ min^{-1} in 700 mbar of oxygen. The used epitaxial thin films samples of dimensions 5×5 mm^2 grown on single crystal of MgO substrate of dimensions 10×10×5 mm^3 are employed (Saleh, Hamam, Said, Abu-Samrah, and Abu-Aljarayesh, 2000).

3.4 Measurements

3.4.1 The Resistivity measurements

Measurements of the resistance, R (or the resistivity ρ) of Al-doped YBCO films versus the temperature is the most principal technique

that can be employed to determine and to test the superconducting state and the transition temperature of a superconductor.

The resistivity measurements can be obtained using the standard four-probe technique. Two leads or probes carry a known constant current, I, into and out of the specimen while the other two leads measure the potential drop, V, between two equipotential surfaces resulting from the current flow. A schematic representation of this technique is displayed in Figure 3.2.

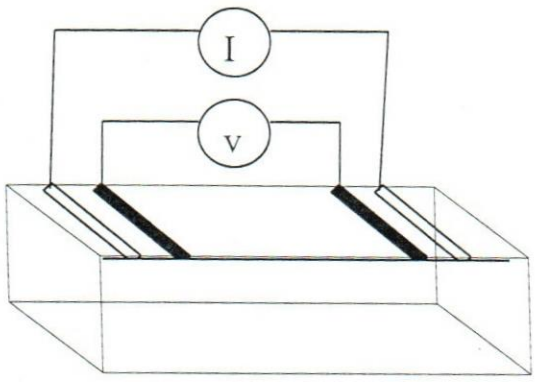

Figure 3.2. Illustration of the standard four-probe resistance measurements technique.

3.4.2 The critical current measurements

There are several methods and techniques used to determine the critical current densities in the superconductors. One of these methods involve the inferences from screening currents associated with measurements of the Meissner effect and produces relatively large values for J_c when applied to single crystal samples. Using the critical field H_c

and the penetration depth λ, the maximum theoretical current density was approximated by (Poole *et al.*, 1988)

$$J_c = \frac{H_c}{3\sqrt{6}\pi\lambda} \qquad (3.1)$$

3.4.3 The magnetization measurements

Many susceptibility and magnetic measurements were performed using a superconducting quantum interferometer device (SQUID) magnetometer. This device can be used as a measuring instrument for both the ac and the dc measurements. More classical techniques such as the vibrating sample magnetometer are also used for susceptibility and magnetization measurements. A dc susceptibility technique is illustrated in Figure 3.3 (Abraham and Keffer, 1971).

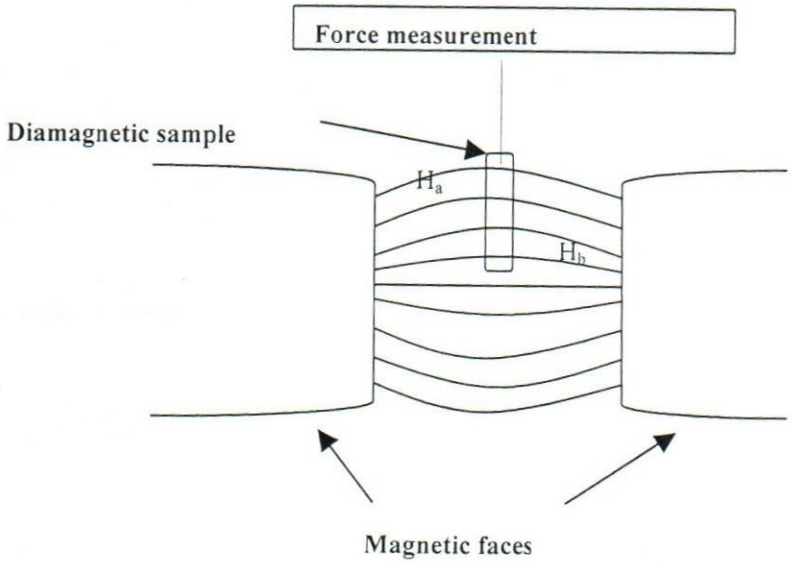

Figure 3.3. Illustration of the dc susceptibility measurement technique.

Magnetization-hysteresis loops were recorded using the vibrating sample magnetometer manufactured by Oxford Instruments in fields up to 12 T. The data were obtained as follows: The sample was cooled to 4.2 K in a zero nominated field, then the hysteresis loops were recorded. The sample was then warmed to a pre-assigned temperature and the hysteresis loop was recorded again. This procedure was repeated at higher temperatures (Slaski *et al.*, 1996).

Magnetization-hysteresis measurements are also performed on polycrystalline samples of YBCO or any high-T_c superconductor ceramics for the purpose of determining J_c. Intergrain and intragrain supercurrent densities may be separated by an inductive technique. This is because there is a large difference in the flux penetration rate into the specimen as a function of field amplitude. The magnetization current density is related to magnetic hysteresis loop through the following expression (James, 1989):

$$J_c = \frac{2\Delta M}{\mu_o D} \tag{3.2}$$

where ΔM is the width of the major hysteresis loop in the M-H curve and D is the thickness of the specimen. As an example of the 0% AL-doped superconducting thin film at 30 K used data, the magnetization data, the complete critical current densities and pinning forces are presented in Appendices A and B, respectively. A typical magnetization loop is

displayed in Figure 3.4. A complete analysis of the same sample collected data will be displayed in Chapter Four.

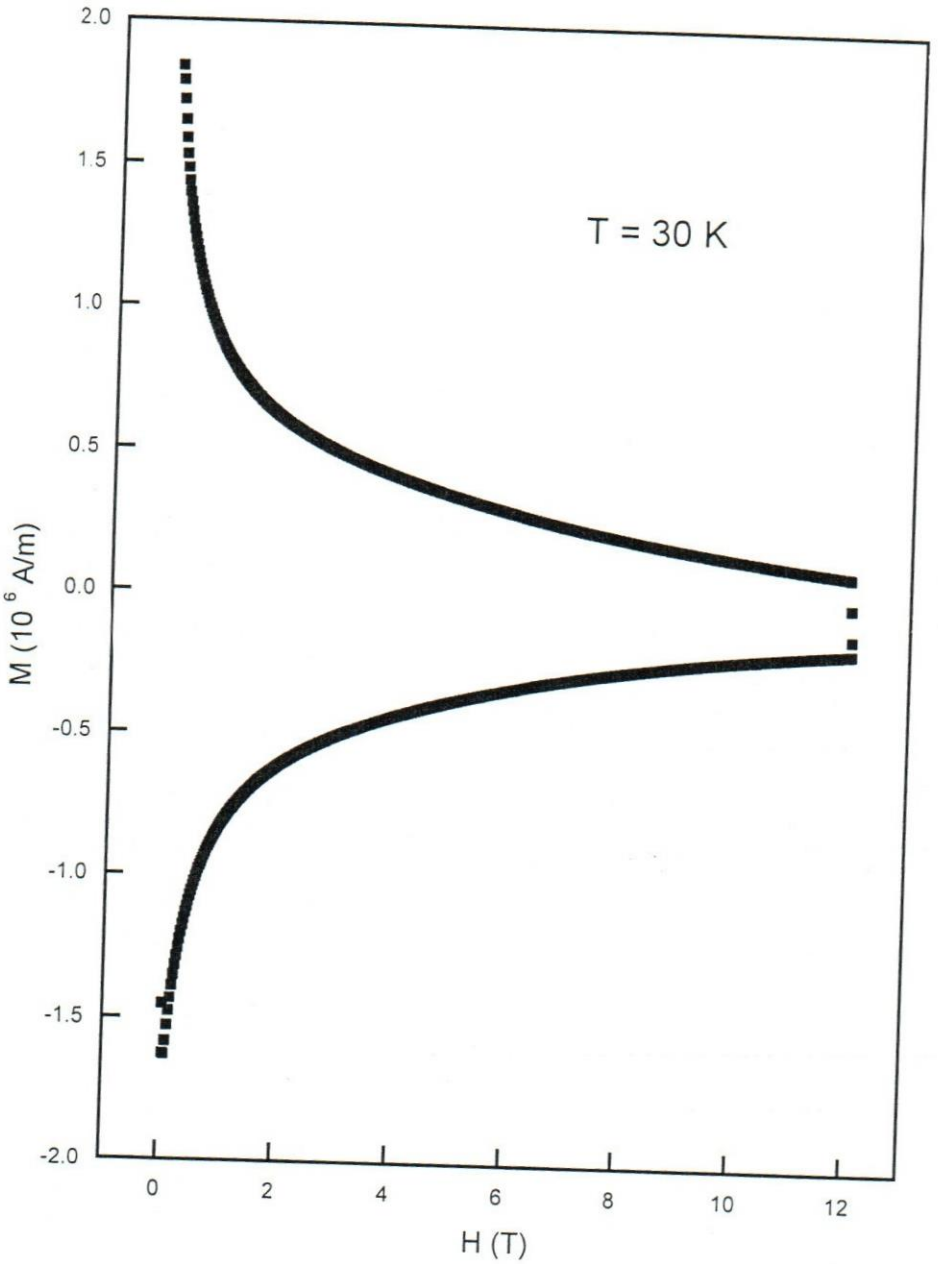

Figure 3.4. A typical magnetization loop

Chapter Four

Results and discussion

4.1 Introduction

The obtained results for Al-doped YBCO superconducting thin films will be analyzed on the basis of the well-known models discussed in Chapter Two. Doping a superconductor with elements will alter its electrical, magnetic and structural properties. The effects of Al doping atoms on critical currents, pinning mechanisms and scaling laws of YBCO superconducting thin films are included.

4.2 Results of magnetization and critical currents

Generally, the critical current of a superconductor decreases as the doping (or impurity) concentration is increased. The variations of transition temperature T_c with Al-doping concentration in YBCO films for different dopant concentrations are displayed in Figure 4.1. It can be seen that below 2% Al, T_c varies slowly with Al-concentration, while above this concentration T_c decreases drastically. For example, around 2% of Al concentration, T_c is around 85 K; while it is 25 K in case of 5% Al concentration (Appendix C). This can be explained by assuming that Al atoms occupy the Cu sites, causing a decreasing in the superconductivity and increasing the resistivity of the normal phase (Kim, Xenikos, Thorns, and Lemberger, 1992).

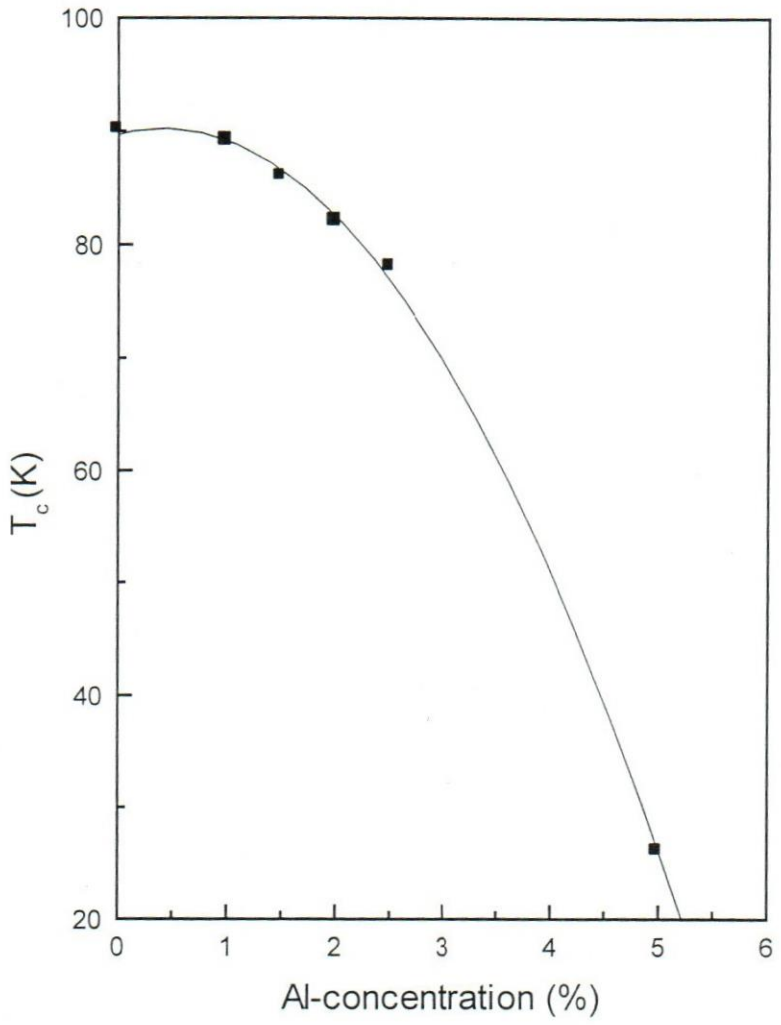

Figure 4.1. Variations of transition temperature T_c with Al-dopant concentration at 0 T applied magnetic field .

As more Al atoms replace the Cu atoms, the transition temperature decreases dramatically because the superconducting CuO planes are distorted. This resulted in an increase of the structure disorder. As a result, the fluxoids pinned in the superconductor affect the different vortex phases (Xenikos, and Lemberger, 1994). The orthorhombic phase is also affected and becomes tetragonal as the dopant concentration

increases. This prediction was tested and the results were confirmed by making use of powder x-ray and neutron diffraction analyses somewhere (Xenikos *et al.*, 1994).

A typical magnetization curves for three Al-doped samples with concentrations 0, 1.5, and 2.5% Al at 30 K are displayed in Figure 4.2. Only one-half of the curve, which is symmetric about the origin, is shown for clarity. The general behavior of the hysteresis loops and their rapid decrease with increasing doping concentration is common for all investigated samples. Also, the width of the hysteresis loop is directly proportional to the critical current density (J_c α ΔM) flowing in the specimen. A typical complete magnetization curve at 79 K for the 1.5 % Al concentration sample is displayed in Figure 4.3.

The shapes of the hysteresis loops at various temperatures are qualitatively similar. Contrary to the results obtained for YBCO single crystal, no fishtail anomaly with a dip in magnetization below a central peak was observed, (Krusin *et al.*, 1992). The fishtail anomaly has been attributed to the presence of oxygen vacancies or dislocation network in the sample (Kim *et al.*, 1995). Similar behaviors were reported for 5% Fe, Co or Ni doped YBCO laser ablated thin films (Song *et al.*, 1992). Generally speaking, the magnetization curves of all samples were found to decrease with increasing dopant concentration.

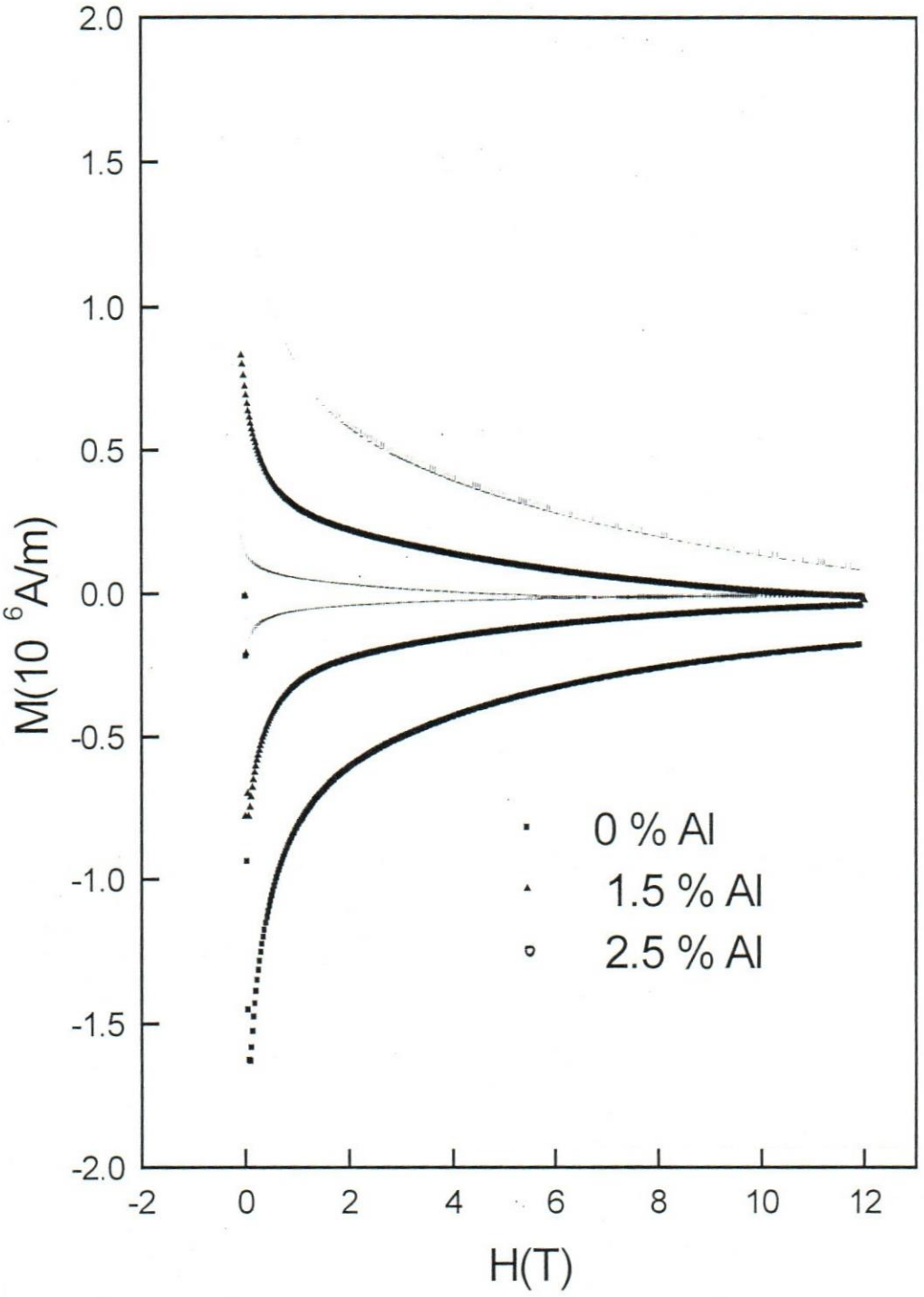

Figure 4.2. Typical magnetization hysteresis loop for three samples with different dopant concentrations at 30 K.

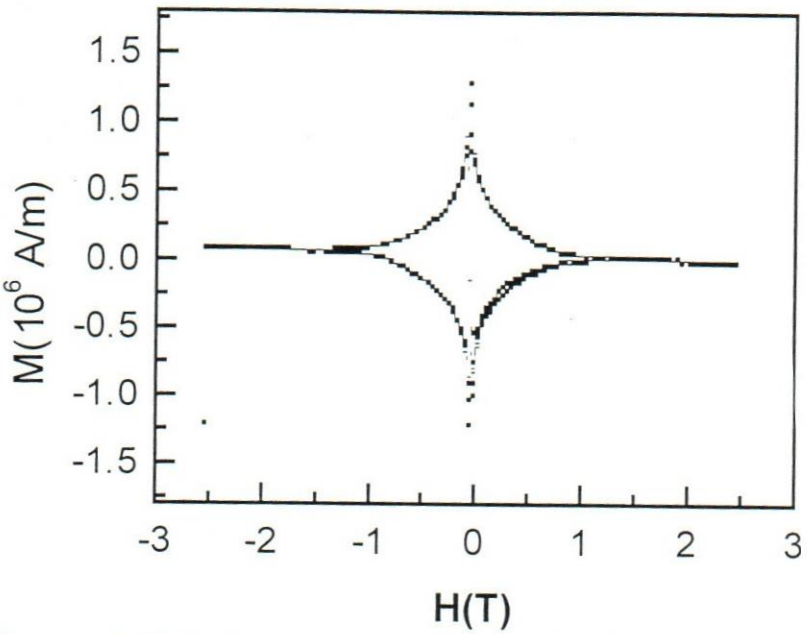

Figure 4.3. Typical magnetization hysteresis loop for 1.5 % Al-doped YBCO superconducting thin film at 79 K .

The magnetization decreases rapidly with applied fields up to about 2 T. At higher fields the magnetization decreases more slowly and almost linear with the applied field (Saleh *et al.*, 2000). Similar results were obtained for the magnetization of $(Y_{1-x}Pr_x)Ba_2Cu_3O_{7-\delta}$ samples with different Pr concentrations (Xiao, 1997). Clearly, for all high-T_c superconductors, there is a similarity in the magnetization loops behavior with different doped elements. This behavior can be described qualitatively well on the basis of the extended critical state model (Xiao, 1997).

The critical current density J_c was calculated using magnetization curves for 0, 1.5 and 2.5% Al-doped YBCO superconducting thin films on the basis of Bean's Critical State Model (Murakami *et al.*, 1992). In case of a long rectangular sample, the current density can be written as:

$$J_c = \frac{20\Delta M}{w[1 - w/3\ell]} \qquad [Am^{-2}] \qquad (4.1)$$

where ΔM is the difference between the upper and lower branches of the magnetization loop, W and ℓ are the width and the length of the rectangular sample. The calculated values of critical current density as a function of temperature for 0, 1.5, and 2.5% are plotted for zero and 1 T applied fields in Figures 4.4 and 4.5, respectively. Similar behavior of J_c versus T was observed for other fields. No saturation of J_c was observed at low temperature, as might be expected for a weakly linked sample (Kramer, 1973). At low concentrations (< 0.5 %), a certain positive effect was observed concerning the critical current density J_c values. In general, all critical current densities at low concentrations are high. This is related to the possibility of partial pinning of Josephson vortices in the "weakly seeded" places on the boundaries (Nurgaliev, Miteva, Nedkov, Veneva, and Taslakov, 1994). All doped ceramics show similar behavior regardless of the dopant elements type. In case of high Al-doped YBCO, a remarkable increase of resistance and a decrease in critical current is

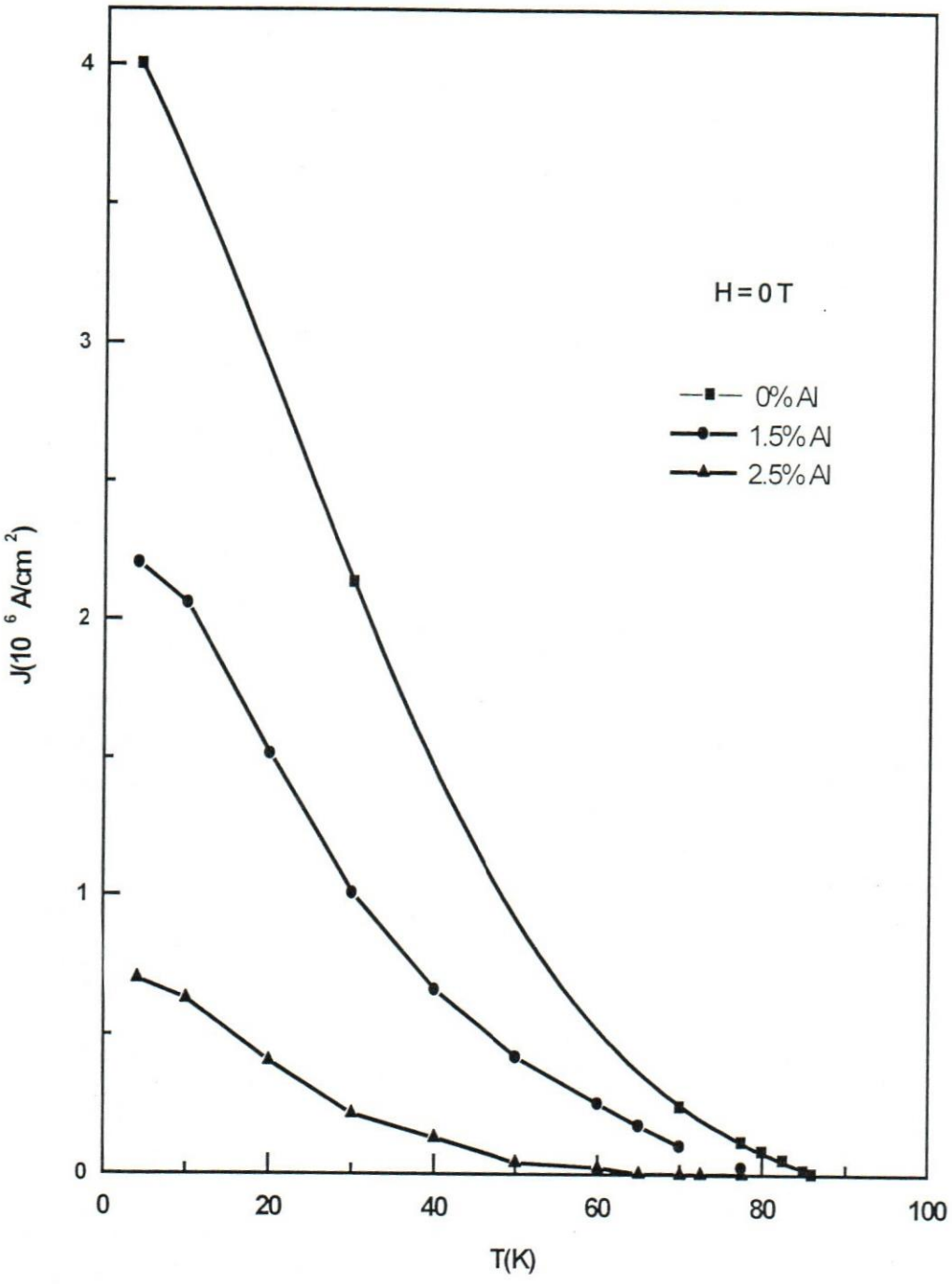

Figure 4.4. The critical current density J_c dependence on temperature for three YBCO samples of different Al concentrations in a zero applied field.

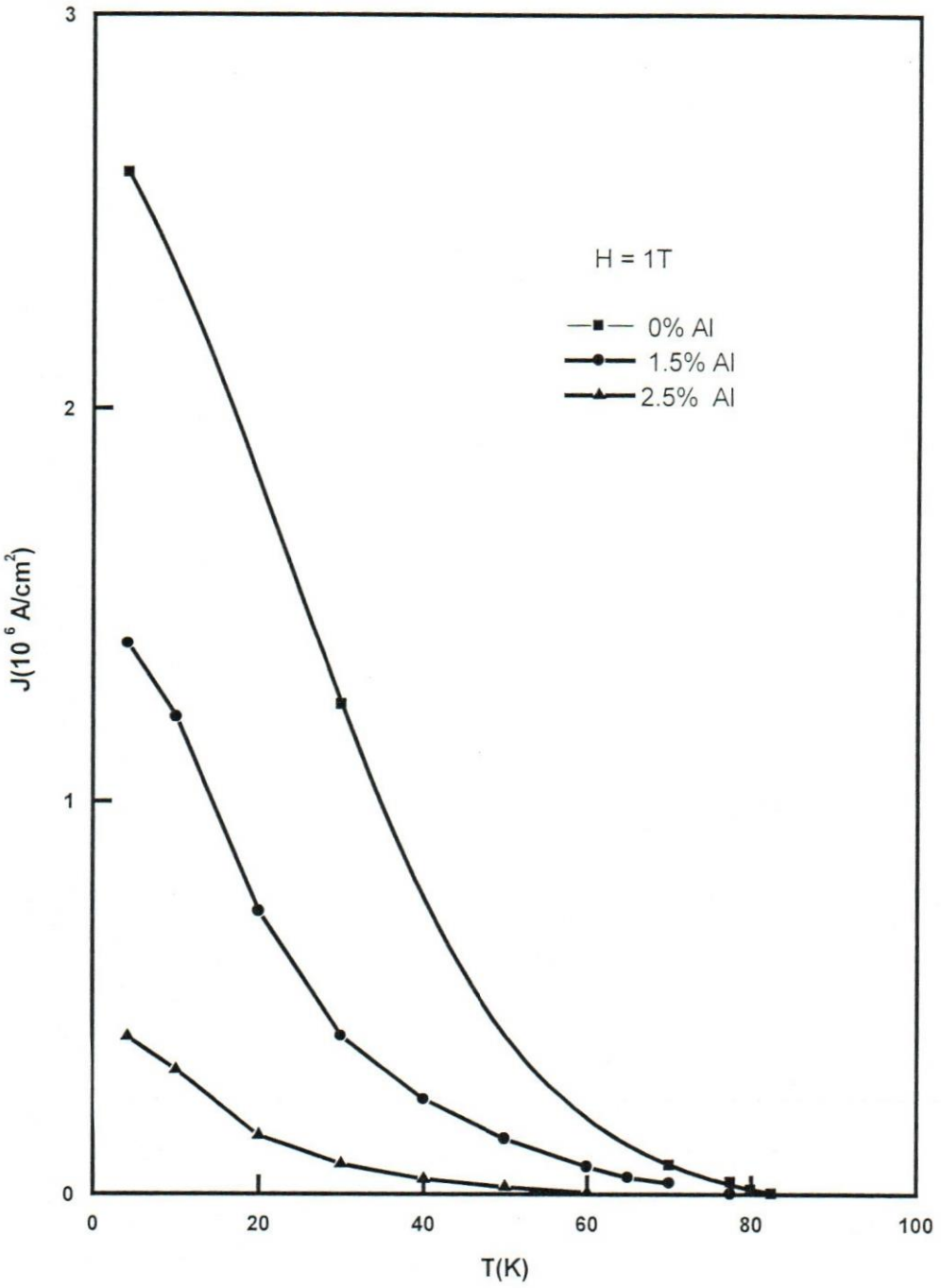

Figure 4.5. The critical current density J_c dependence on temperature for three YBCO samples of different Al concentrations in a 1 T applied field.

observed, while at low concentration (less than about 1.5%) this observation becomes unremarkable (Saleh *et al.*, 2000).

The critical current density decreases by increasing the applied magnetic field for low dopant concentration (Figures 4.4 and 4.5). This type of behavior is expected for this type of doped superconductors, where the substituted atoms replace the Cu sites. The dopant atoms not only destroy the CuO superconducting planes, but also change the crystal structure (Slaski *et al.*, 1996). At higher temperatures the dependence of J_c on magnetic field is much slower. Similar observations were obtained for Fe or Ni-doped YBCO superconducting thin films by means of magnetization measurement or transport measurement (Neil, 1992) and for Na-doped YBCO superconducting thin films (Nurgaliev *et al.*, 1994).

The reduced critical current density j ($J_c(T)/J_c(0)$) as a function of reduced temperature t (T/T_c) for the films at 0 and 1 T is displayed in Figure 4.6 and Figure 4.7, respectively. These data can fit a power law of the form

$$j = (1 - t)^n \qquad (4.2)$$

where the exponent n has a typical value of the order of 2.3. This scaling is in a good qualitative agreement with J_c data obtained for epitaxial Bi-2212 thin films (Kim *et al.*, 1995) and for YBCO discs (Ji *et al.*, 1997).

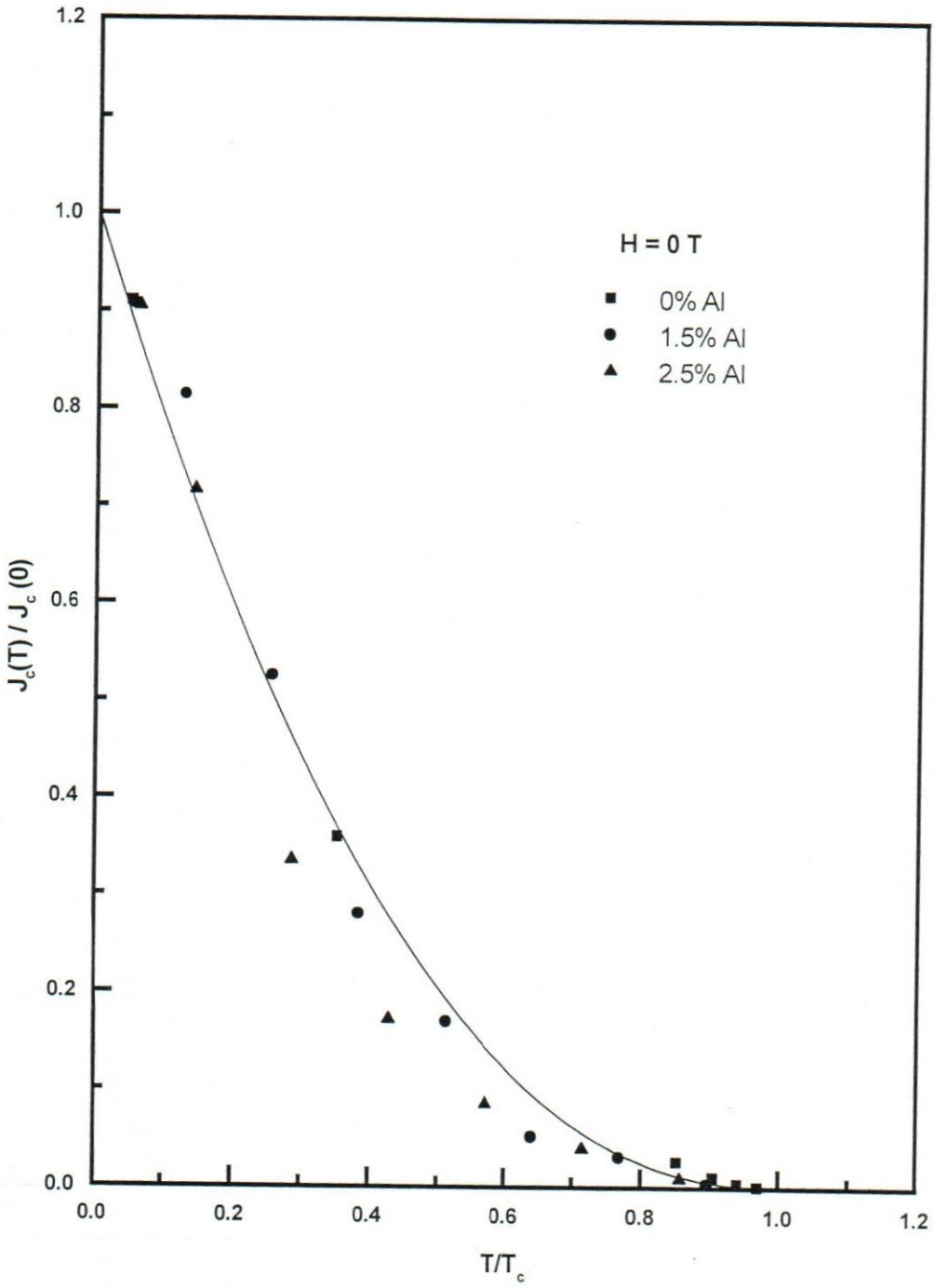

Figure 4.6. The reduced critical current density for different concentrations at 0 T magnetic field as a function of the reduced temperature.

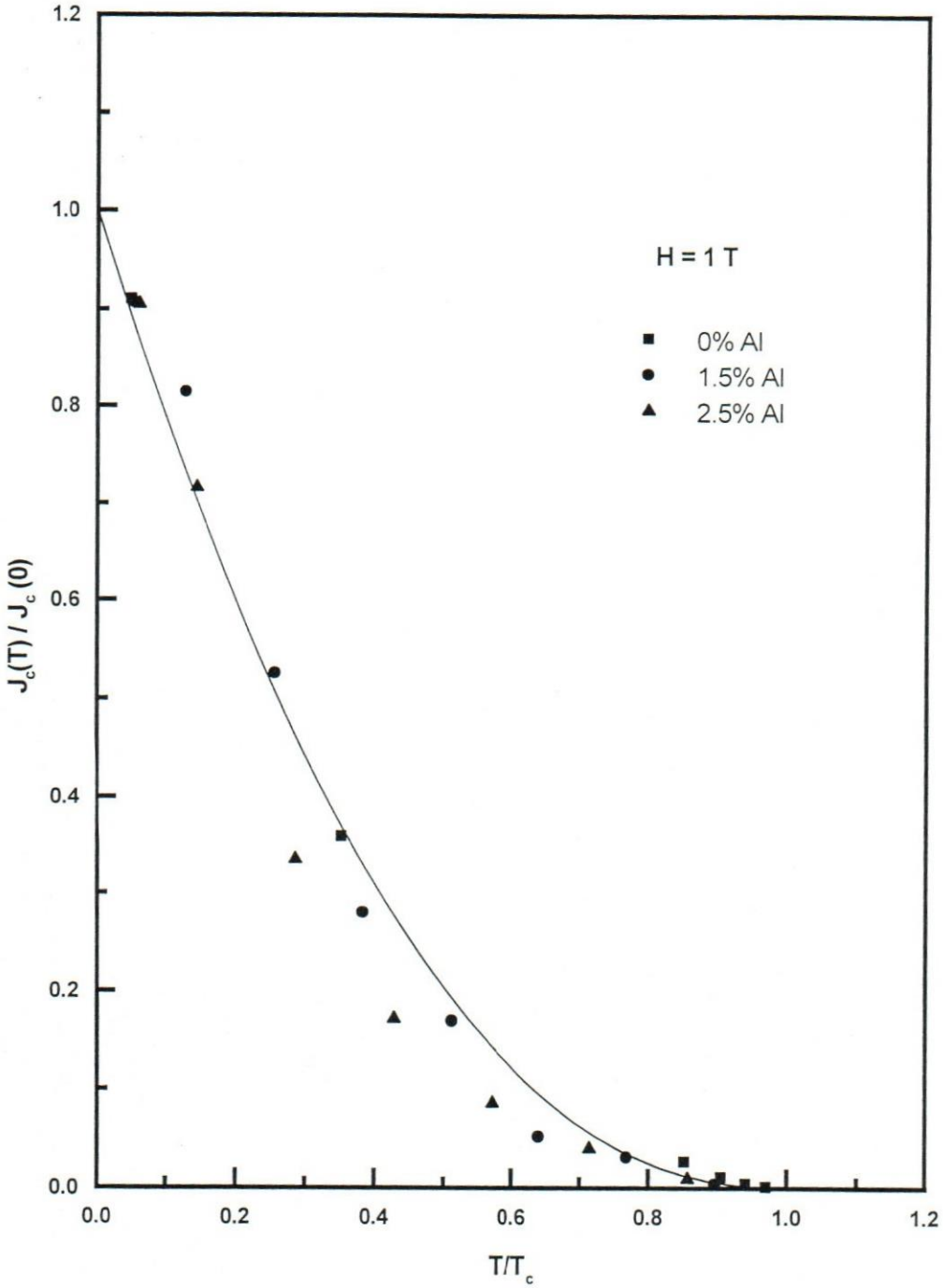

Figure 4.7. The reduced critical current density dependence on reduced temperature for different concentrations at 1 T magnetic field.

The scaling law of equation (4.2) allows us to estimate the critical current at T = 0 K in general.

The estimated values of the current densities at zero applied magnetic field for the 0%, 1.5% and 2.5% Al-doped YBCO superconducting samples are 4.60×10^{6} A cm^{-2}, 2.31×10^{6} A cm^{-2} and 2.10×10^{6} A cm^{-2}, respectively. These results can be interpreted in terms of the extended Bean critical state model (Xiao, 1997).

The critical current density scaling law for the various YBCO samples of different dopant concentration suggests that the dynamical mechanism of vortex motion in Al-doped YBCO samples can be quantitatively described by the collective pinning theory (Krusin *et al.*, 1992). Also, as it could be seen from Figure 4.6, the addition of Al to YBCO samples, up to highest level in our study, did not influence the scaling approach itself.

In order to get more information about the relevant pinning mechanism, another important scaling law for conventional hard type-II superconductors known as the volume pinning force scaling law can be examined. The pinning force is related to current density and applied field through the relation:

$$\vec{F}_p = \vec{J}_c \times \vec{H}\,, \qquad \mathrm{N/m^3} \qquad (4.3)$$

The J_c values are calculated from the magnetization loop according to equation (4.1), while the H values obtained from the magnetization curves were used to calculate the pinning force according to equation (4.3). The reduced pinning force can be introduced as:

$$f = \frac{F_p}{F_{max}} \tag{4.4}$$

where F_{max} is the maximum force observed at a given temperature. The reduced field, h, can also be defined as:

$$h = \frac{H_p}{H_{max}} \tag{4.5}$$

where H_{max} is the corresponding maximum magnetic field. Therefore, the reduced pinning force could be scaled well with a relation of the form;

$$f \propto h^p(1-h)^q \tag{4.6}$$

Figures 4.8 - 4.13 display the reduced pinning force f_p against the reduced field for the three samples with Al concentration, 0%, 1.5%, and 2.5% at different temperatures. Obviously, the reduced pinning force displayed in Figures 4.8 - 4.13 fit well at temperatures near T_c (Appendix C) the scaling law presented in equation (4.6). The exponents p and q were found to have values of: p = 0.70±0.01 and q = 1.86±0.05 for the 0% Al-doped sample, p = 0.68±0.01 and q = 1.60±0.02 for the 1.5 % Al-doped sample, while p = 0.67±0.02 and q = 1.87±0.01 for the 2 .5% Al-doped sample. The errors were estimated using the general least squared fit

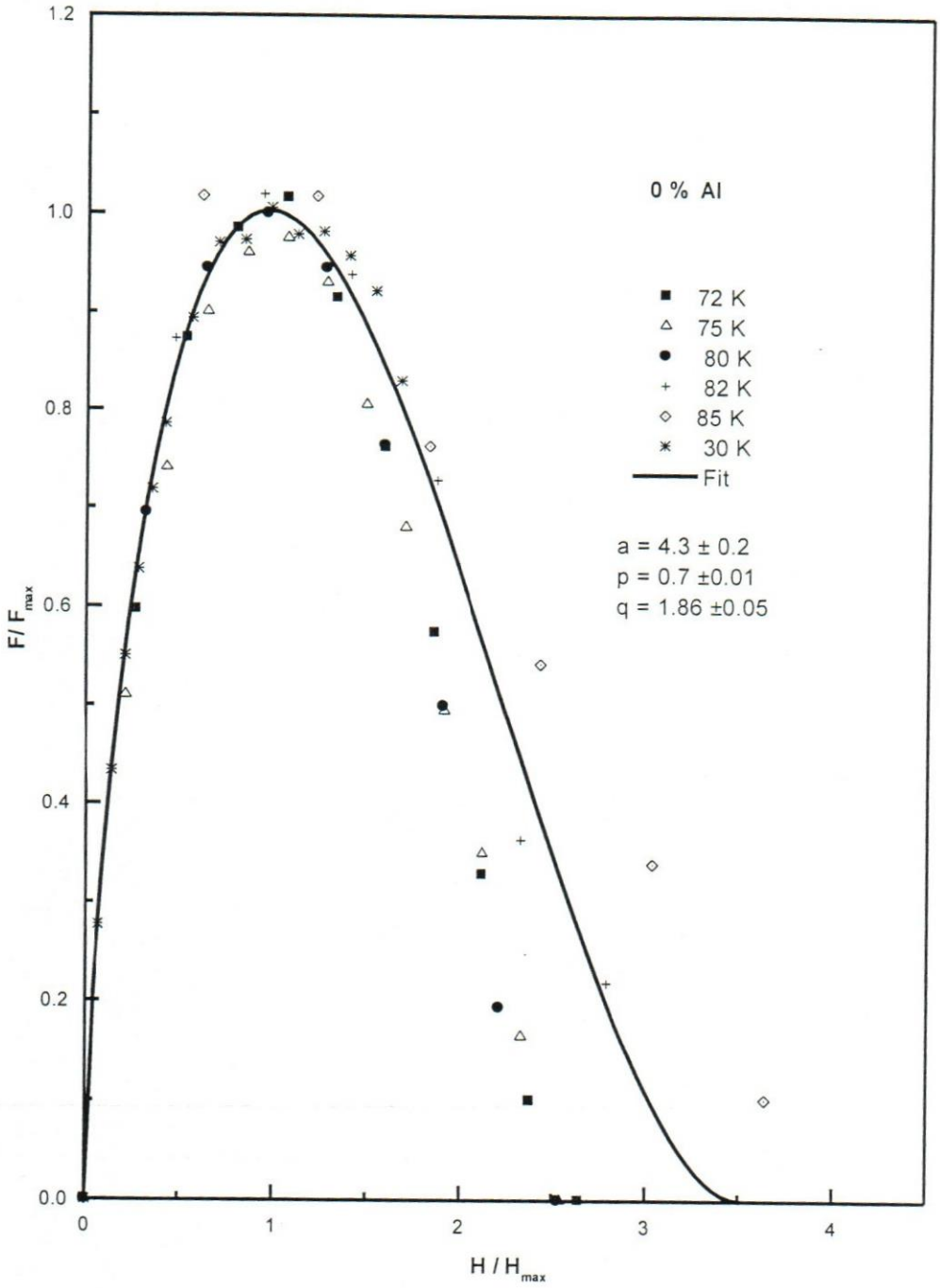

Figure 4.8. The reduced pinning force as a function of the reduced field for a 0% Al-doped sample at various temperatures.

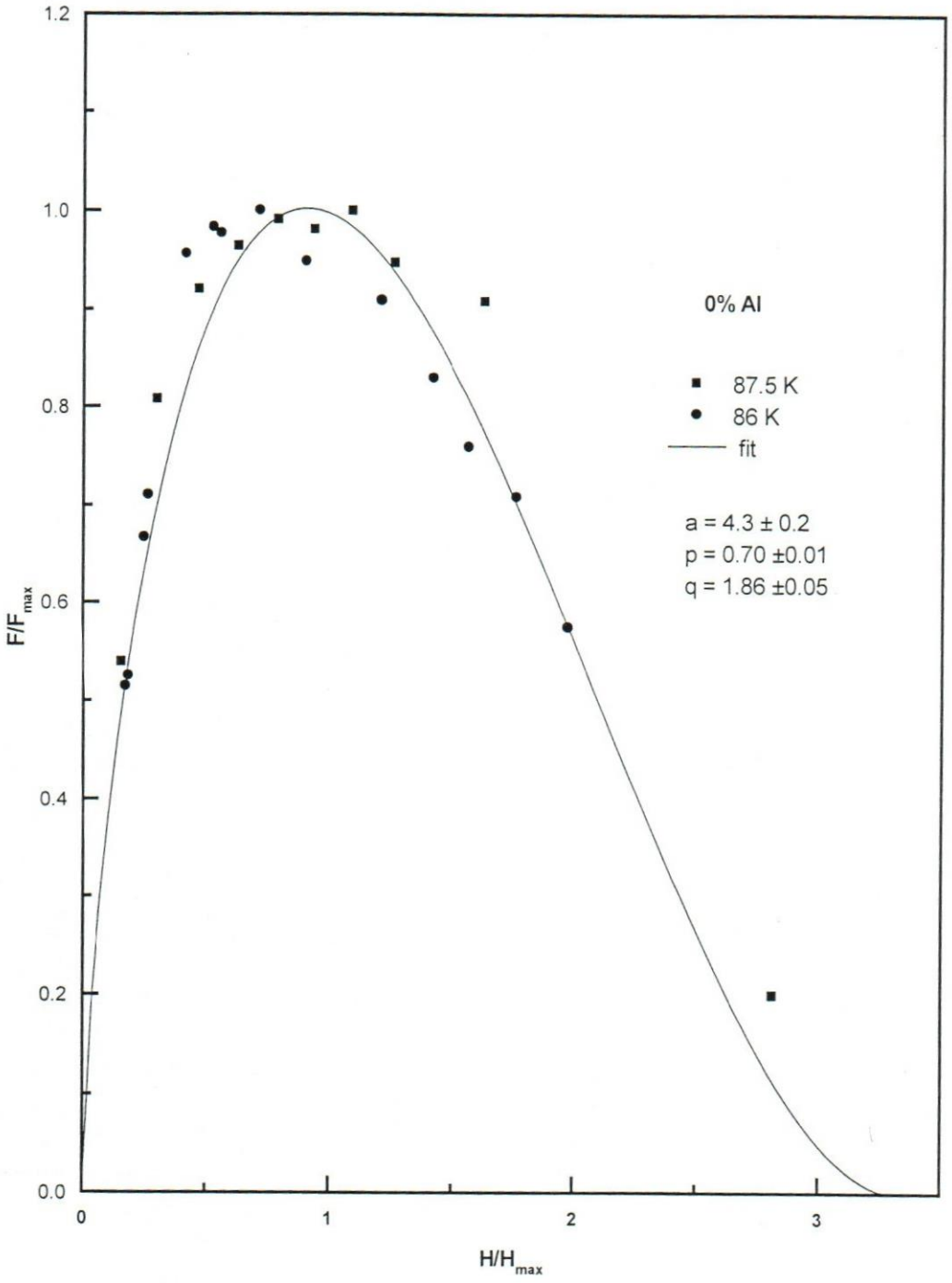

Figure 4.9. The reduced pinning force as a function of the reduced field for a 0 % Al-doped sample at temperatures near the transition temperature.

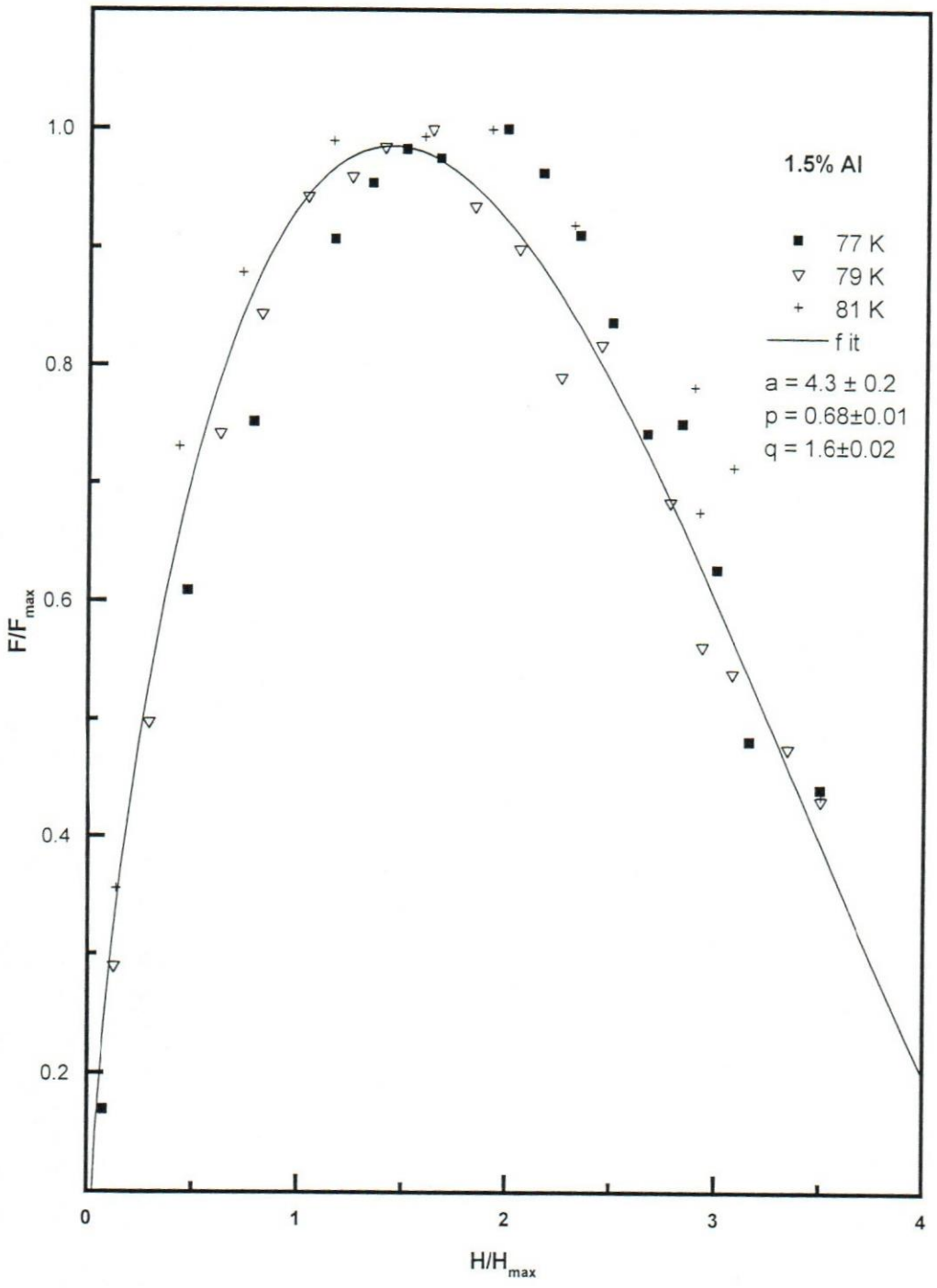

Figure 4.10. The reduced pinning force as a function of the reduced field for a 1.5% Al-doped sample at different temperatures.

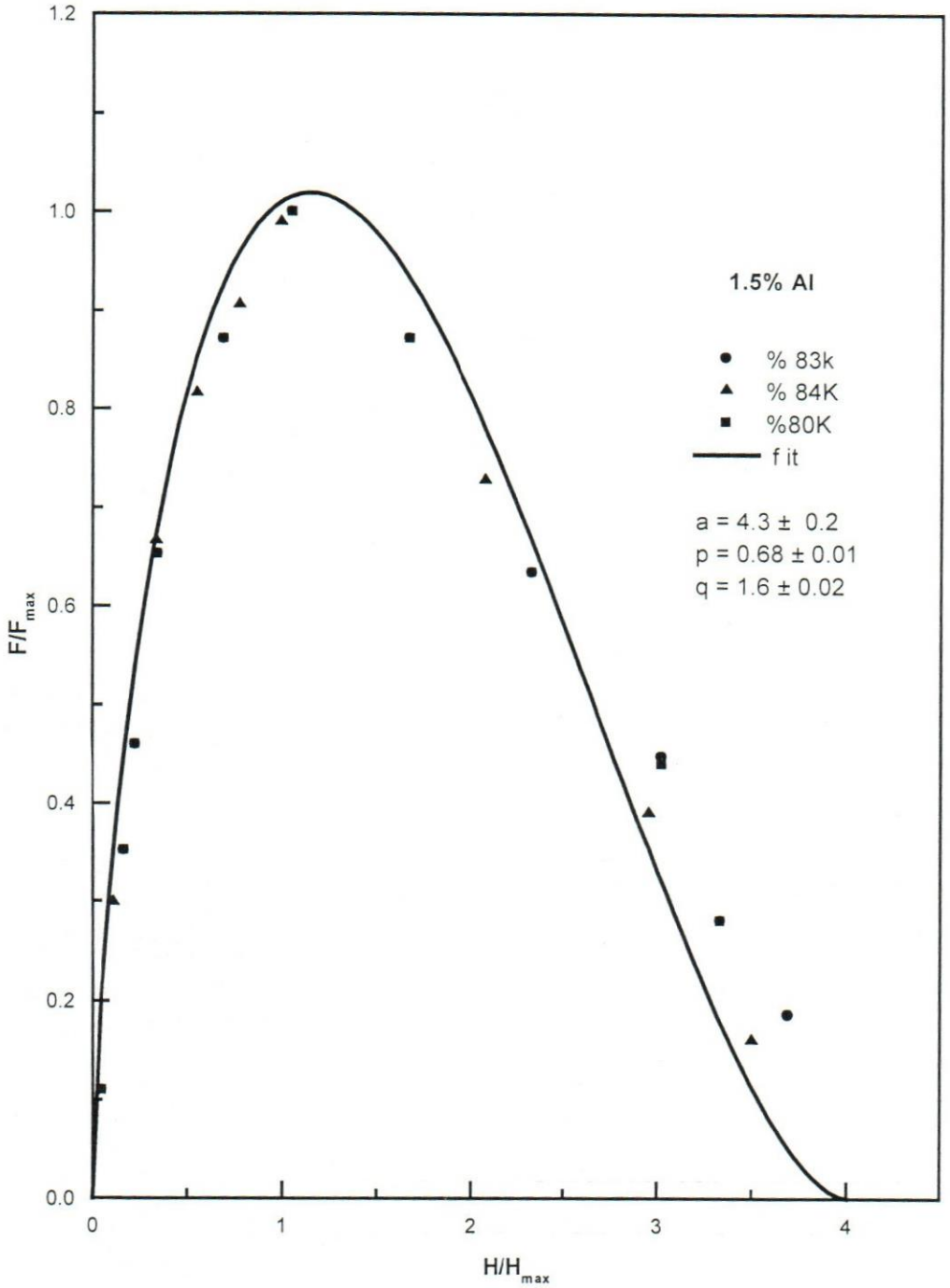

Figure 4.11. The reduced force as a function of the reduced field for 1.5% Al-doped sample at temperatures near the transition temperature.

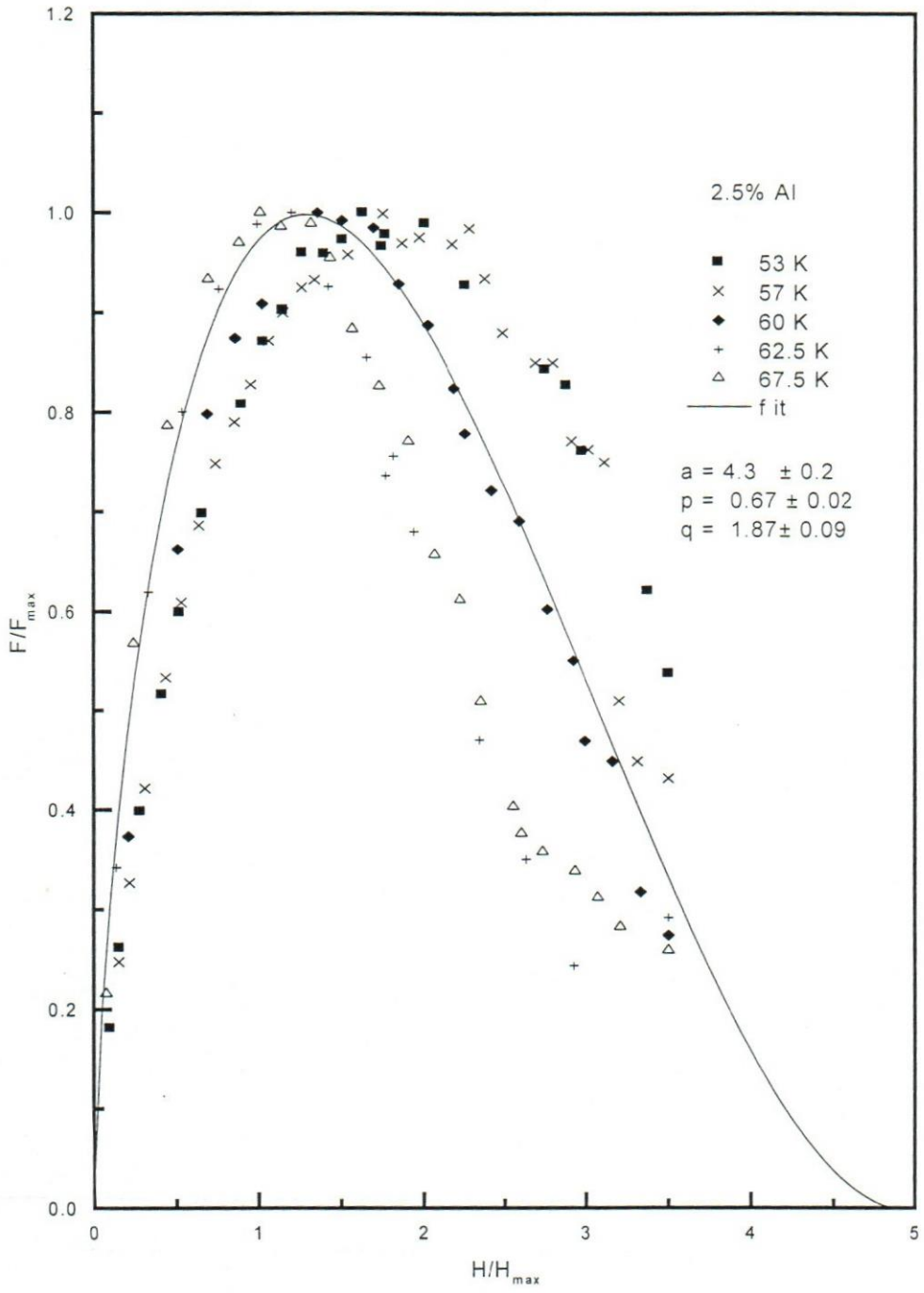

Figure 4.12. The reduced pinning force as a function of the reduced field for a 2.5% Al-doped sample at various temperatures.

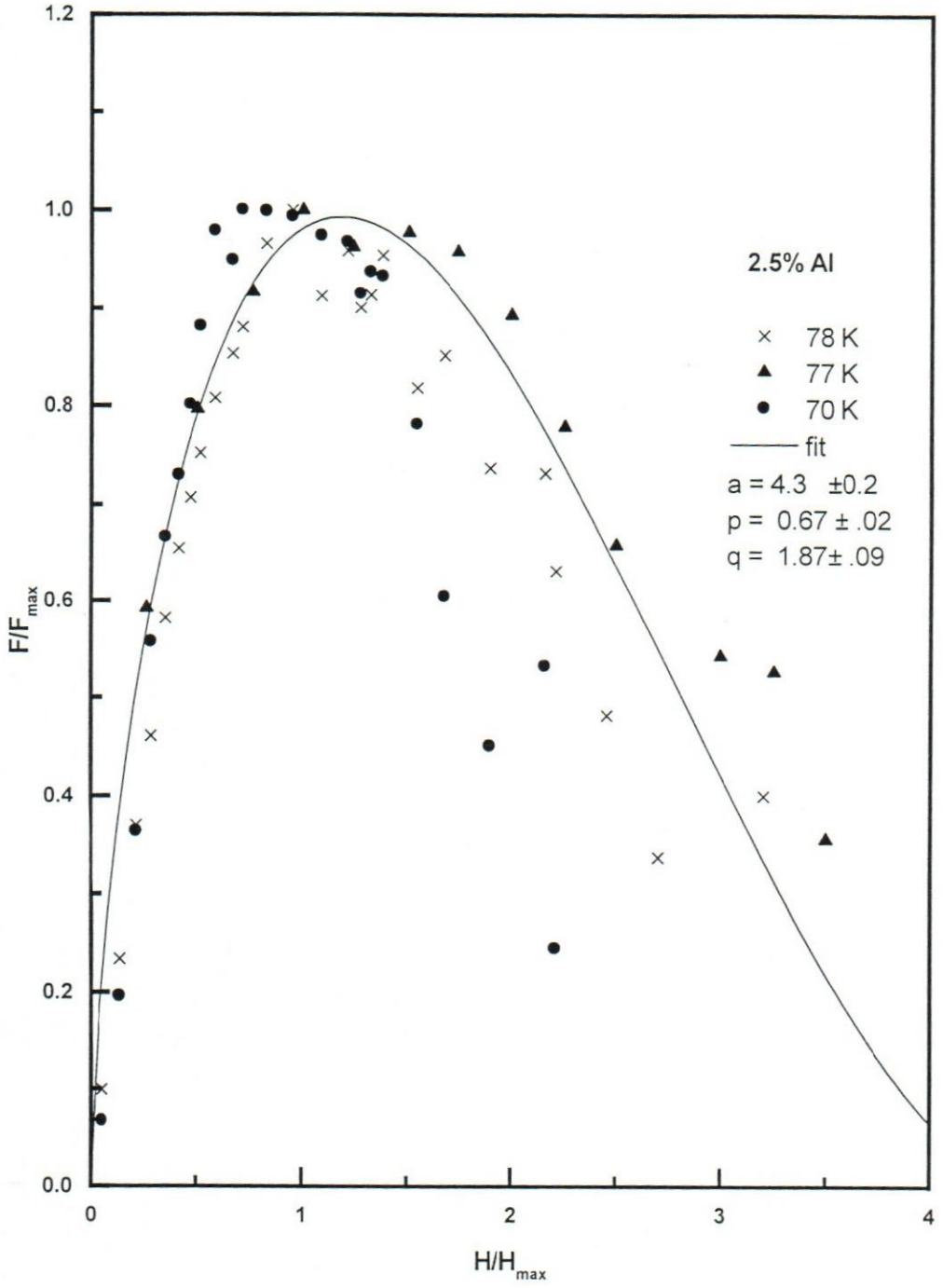

Figure 4.13. The reduced force as a function of the reduced field for a 2.5% Al-doped sample at temperatures near the transition temperature.

method. The obtained results concerning the scaling law in equation (4.6) are found to be in reasonable agreement (8%) with the flux-line lattice (FLL) shear model (Kramer, 1973) and similar to that obtained for YBCO single-crystal superconductors (Civale *et al.*, 1991).

To check the validity of the scaling for samples with different concentrations, the reduced force versus the reduced field was plotted in Figures 4.14 and 4.15 for three samples of 0%, 1.5% and 2.5% Al-dopant concentration at T = 30 K, and 77 K, respectively. The presented results are also in good qualitative agreement with conventional superconductors (Kramer, 1973) with exponent parameters of p = 0.70±0.02 and q = 1.72±0.01, (the sum p + q = 2.42). The fact that all three samples with different dopant concentrations can be scaled using the same formula suggests that the dopant concentration does not affect the pinning mechanism even though it affects the structure and increases the disorder within the sample (Xenikos *et al.*, 1994).

The fact that the peak value of the reduced force occurs at almost the same value of the reduced field regardless of the temperature under consideration suggests a scaling law of the form

$$F_{max} = f(h)H_{max}^{n} \qquad (4.7)$$

where f(h) is a function of the reduced field and n is a parameter that can be extracted from the slope of log F_{max} versus log H_{max} plot.

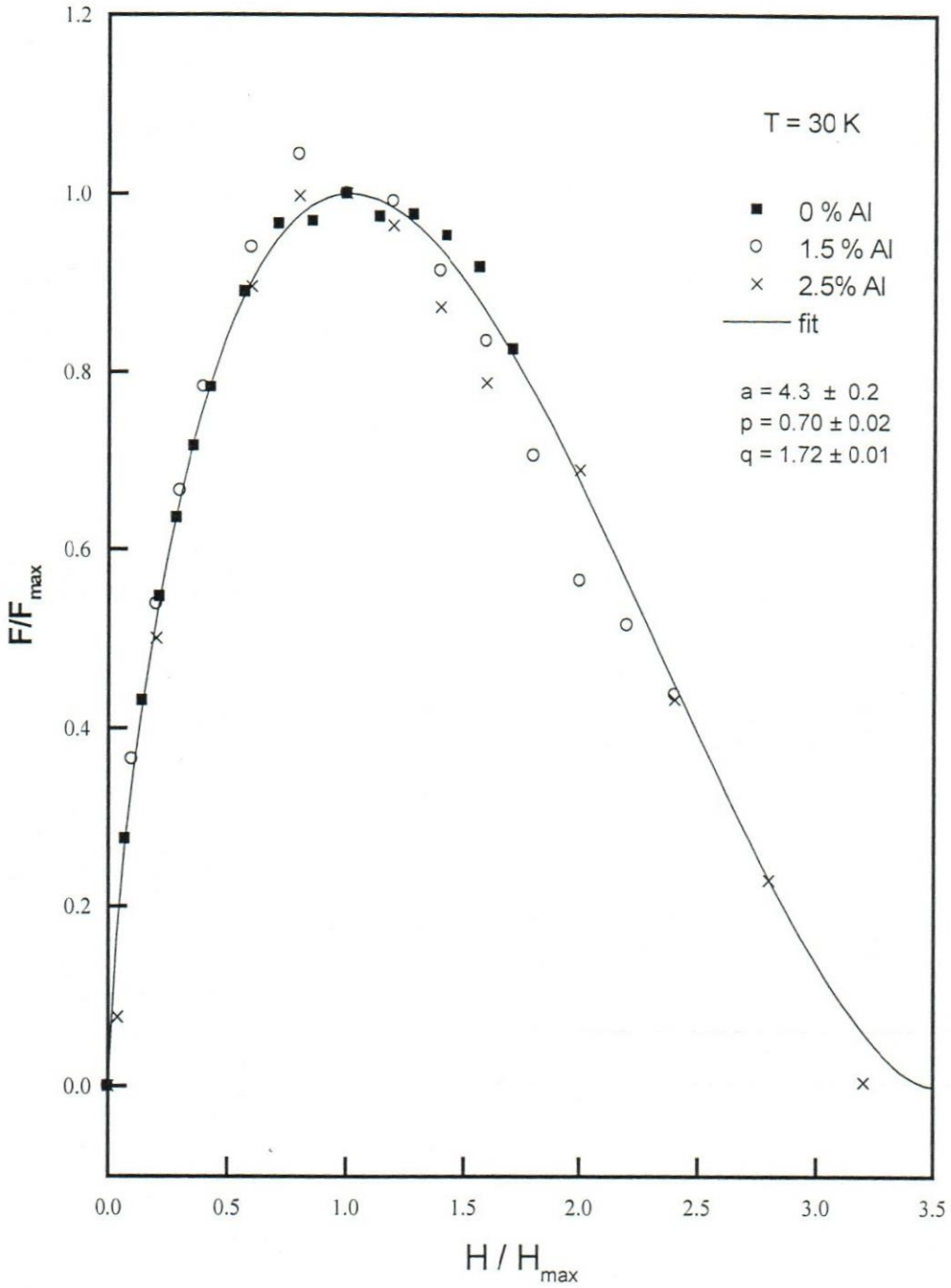

Figure 4.14. The reduced pinning force for 0, 1.5, and 2,5 % Al-doped sample as a function of the reduced field at 30 K.

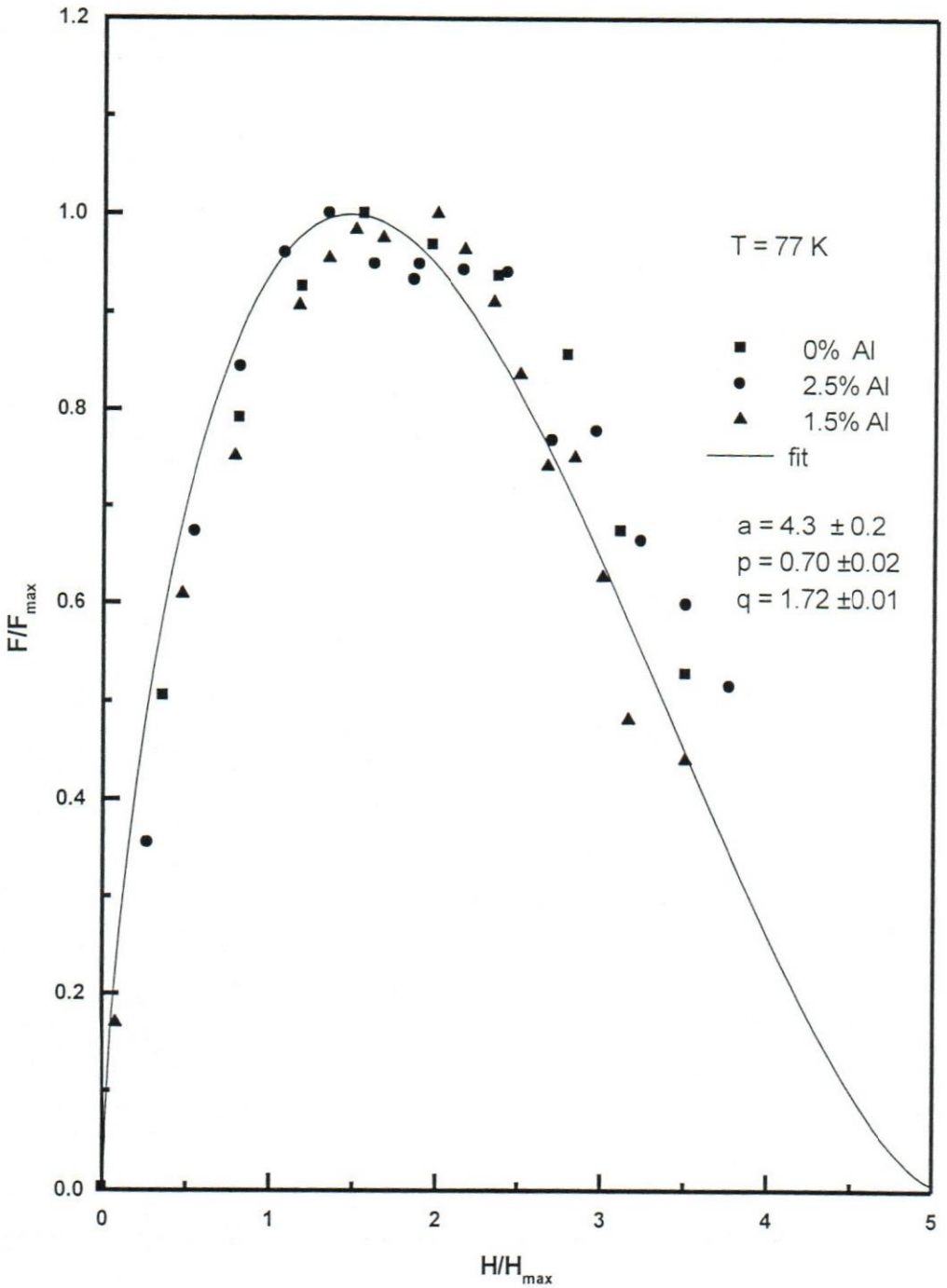

Figure 4.15. The reduced pinning force for 0, 1.5, 2.5% Al doped samples as a function of the reduced field at 77 K.

The maximum pinning force at various temperatures is plotted against the corresponding maximum field for the three samples of different concentrations in Figure 4.16. These data were scaled very well to a relation of the form

$$F_{max} \propto H_{max}^{2.43} \qquad (4.8)$$

It can be shown that scaling law of the form given by equation (4.8) can be rewritten as:

$$F_{max} \sim H_{max}^{p+q} \qquad (4.9)$$

The estimated exponent in the present work is very close to a value of 2.5 This value is close enough to the predicted exponent parameter (n) value predicted for p and q exponents belonging to conventional low-temperature superconductors (Kramer, 1973). Such type of scaling seems to be applicable to all type-II superconductors regardless of their structure or their upper critical field.

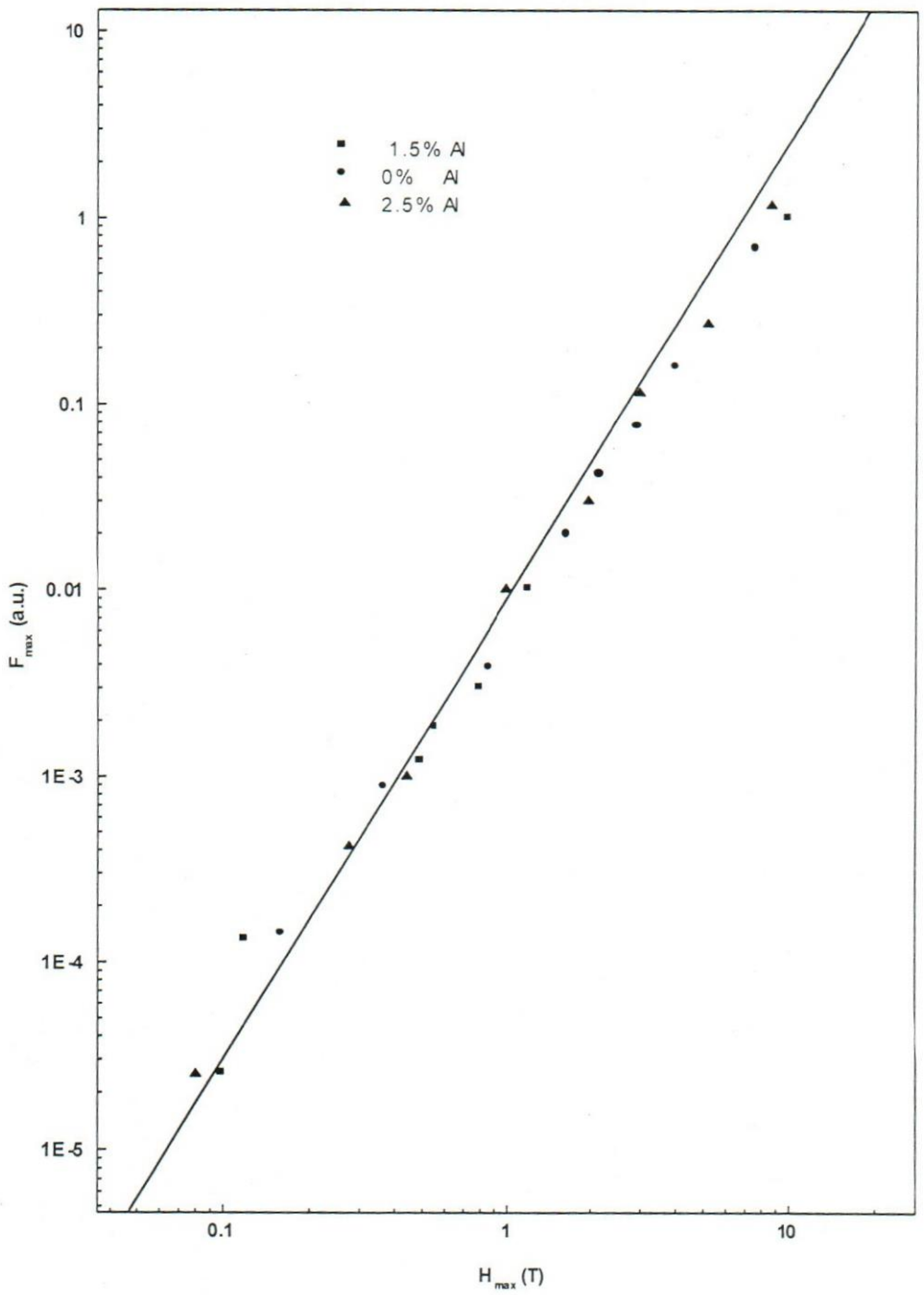

Figure 4.16. The maximum pinning force dependence on the maximum field at various temperatures plotted on a log-log scale.

Chapter Five

Summary and Future work

Pinning centers are one of the important factors affecting J_c in high-T_c superconductor materials. As it could be seen from the results in Chapter Four that, T_c varies slowly with Al-concentration. This could be explained by the fact that Al atoms occupy the Cu sites, causing a decrease in superconductivity and an increase in the resistivity of the normal phase. As more Al atoms replace the Cu atoms the transition temperature decreases dramatically.

The magnetization curves of Al-doped YBCO laser ablated thin films around the critical temperature in fields of up to 12 T showed no anomalous behavior for any of the samples investigated and they are well fitted with the scaling laws of Bean critical state model. The current density J_c decreased rapidly with increased dopant concentration and the reduced current density scales to a relation of the form $j \propto (1-t)^n$ where $n \sim 2.3$.

The pinning force density for all samples is also scaled as $F_p \propto h^p(1-h)^q$, with p ~0.70 ± 0.02 and q ~1.72 ± 0.05 around the critical temperature for all samples. The scaling laws are in a good agreement with Kramer's flux- lattice line (FLL) shear model fundamental model.

The maximum pinning force density at a given temperature F_{max} scaled to a power law $F_{max} \propto H_{max}^{n}$ with n~2.5 consistent with the values of p and q derived from the scaling laws for conventional superconductors. This type of scaling seems to fit to all type-II superconductors regardless of their structure or their upper critical field.

The work presented in this thesis can be extended to include the effects of thin films thickness, magnetic relaxation, current density relaxation, and transport phenomenon for Al-doped YCBO superconducting thin films.

References

Abilio C. C., Loureiro S. M., Capponi J. J., and Gorinho M., (1995), Physica C **245**, p. 1

Abrahams E., and Keffer F., (1971), **McGraw-Hill Encyclopedia of Sience and Technology,** Vol. **13**, (McGraw-Hill, New York) pp. 348-349.

Ashcroft N. W., and Mermin N. D., (1976), **Solid State Physics**, (Saunders Company, New York).

Bednorz J. G., and Muller K. A., (1986), Z. Phys. B **64**, p. 189.

Campbell A. M., and Evetts J. E., (1972), Adv. Phys. **21,** p. 372.

Chen X. D., Sang Y. L., Golbeng J. P., Sung I. L., McMichael R. D., Gaincs, (1987), Rev Sci, **58** pp. 1565-1571.

Civale L., McElfresh M. W., Marwick A. D., Holtzberg F., and Field C., (1991) , Phys. Rev. B **43**, p. 13732.

Dew-Hughes D., (1974), Phil Mag. **30**, p. 293.

Fietz W. A., and Webb W. W., (1969), Phy. Rev. **178,** pp. 657-667.

Gupta A., Tuset E. D., Kakut M. G., and Fossheim F., (1996), Physica C **272**, p. 33.

Hermann A. H., Sheng Z. Z., Kiehl W., El-Ali A., Hambourger P., Almassan, D., Estrada C., and Data. T. (1988), J. Appl. Phys. **64,** p. 5050.

James D. D., (1989), **Engineer's Guide to High-Temperature Superconductors,** (John Wiley & Sons, New York).

Ji Z. M., Geng J. F., Chen W. M., Yu H. X., Sun A. M., Chen Q. H., Yang S. Z., and Jin X., (1997), Physica C **279**, pp. 233-240.

Kalyanaraman R., Oktyabrsky S., and Narayan J., (1995), Appl. Phys. **85,** p. 6636.

Kim J-Tae., Xenikos D. G., Thorns A., and Lemberger T. R., (1992), Appl. Phys. **72**, p. 803.

Kim S. F., Li Z. Z., and Raffy H., (1995), Physica C **244** , p.78.

Kittel C., (1996), **Introduction to Solid State Physics**, 7th edition (John Wiley, New York).

Kramer E., (1973), J. Appl. Phys. **44** , p. 1360.

Krusin-Elbaum L., Civale L., Vinokur M. V., and Holtzberg F., (1992), Phys. Rev. Lett. **69** , p. 2280.

Kung P. J., McHenry M. E., Maley M. P., Kes P. H., Laughlin D. E., and Mullins W. W., (1995), Physica C **249,** p. 53.

Li J. N., de Boer F. R., Roeland L. W., Kadowaki M. J. V., Menovsky K.A. A., Feanse J. J. M., (1990), Physica C **169,** pp. 81-86.

Murkami M., (1992), Supercond. Sci. Technol. **5**, pp. 185-203.

Murakami M., Yamaguchi K., Fujimoto H., Nakmura N., Taguchi T., Koshizuka N., and Tanaka S.,(1992), Cryogenics **32**, p. 930.

Niel L., (1992), Cryogenics **32**, p. 975.

Nurgaliev T., Miteva S., Nedkov I., Veneva A., and Taslakov M. J., (1994), Appl. Phys. **76**(10), p. 7118

Obara H., Sawa A., and Kosaka S., (1994), Phys. Rev. B **49**, p. 1224.

Oussena M., de Groot P. A., Marshall M., and Abell J. S.,(1994), Phys. Rev. B **49,** p. 1484.

Pan V. M., Gaponov S. V., Kaminsky G. G., Kuzin D. V., Matsui V. I., Prokhorov V. G., Strikovsky M. D., and Tretiachenko C. G., (1989), Cryogenics, **29**, p. 392.

Poole P., Datta T., and Franch A., (1988), **Copper Oxide Superconductors,** (John Wiley, New York).

Pruymboom A., Kes P. H., Van der Drift E., and Radelaar S., (1988), Phy. Rev. lett. **60,** p. 1430.

Reitz R., Frederick J., Milford R., Christy W., (1993), **Foundations of Electromagnetic Theory,** 4th edition (John Wiley, New York).

Robert W. D., and Richard H. K., (1994), **A Teacher's Guide to Superconductivity for High School Students**, (John Wiley, New York).

Rose I. C., and Rhoderick, E. H., (1978), **Introduction to Superconductivity**, (BPC Wbeatons Great Britain).

Saleh A. M., Hamam Y. A., Said M. R., Abu-Samrah M. M., and Abu-Aljarayesh I., (2000), Supercond. Sci. Technol. **13,** pp. 1607-1611.

Shi Z. X., Ji H. L., and Yao X. X., (1993), Physica C **215**, pp. 439-444.

Slaski M., Woodall P., Wellhofer F., Yeadon M., and Gourgh C. E., (1996), Proceeding of the 8th International Workshop on Critical Currents in superconductors, Kitakyushu, Japan, pp. 27-29.

Song L. W., Yang M., Chen E., and Kao Y. H., (1992), Phys. Rev. **45**, p. 3083.

Tinkham M., (1996), **Introduction to Superconductivity,** 2nd edition (McGraw-Hill, New York).

Wen H. H., Rong X. S., Yin B., Che G. C., and Zhao Z. X., (1995), Physica C **242**, p. 365.

Wu M. W., Ashburn J. R., Trong C. J., Hor P. H., Meng R. C., Gao L., Huang Z. J., Wang Y. Q., and Che C. W., (1987), Phy. Rev. lett. Vol **58**, No. 9, pp. 908-910.

Xenikos D. G., and Lemberger T. R.,(1994), Physica B **194-196**, p. 1913.

Xiao Y. G., (1997), J. Appl. Phys. **81**, p. 5.

Zeng D. C., Liu Z. Y., Zhou G. F., Wang Y. Z., de Boer F. R., and Qiao G. W., (1997), J. Appl. Phys. **81,** p. 4253.

Appendix A

Table 1. Magnetization data For YBCO thin film at 30 K and 0% Al

Time(s)	H(T)	M(A/m)	T(K)	Time(s)	H(T)	M(A/m)	T(K)
0.824	12	-0.1311	30	82.581	10.74	0.1194	30
2.142	11.98	-0.0206	30	84.009	10.71	0.1201	30
3.459	11.96	0.0881	30	85.437	10.69	0.1206	30
4.833	11.94	0.0899	30	86.92	10.67	0.1213	30
6.315	11.92	0.0903	30	88.431	10.64	0.1218	30
7.826	11.9	0.0908	30	89.914	10.62	0.1224	30
9.309	11.87	0.0913	30	91.397	10.6	0.1231	30
10.819	11.85	0.0918	30	92.88	10.58	0.1237	30
12.302	11.83	0.0923	30	94.363	10.55	0.1243	30
13.785	11.8	0.0929	30	95.846	10.53	0.1249	30
15.268	11.78	0.0934	30	97.274	10.51	0.1256	30
16.696	11.76	0.0939	30	98.757	10.48	0.1263	30
18.179	11.74	0.0946	30	100.213	10.46	0.1268	30
19.635	11.71	0.0951	30	101.641	10.44	0.1275	30
21.118	11.69	0.0955	30	103.124	10.42	0.1281	30
22.545	11.67	0.0961	30	104.552	10.39	0.1287	30
24.028	11.65	0.0966	30	105.98	10.37	0.1294	30
25.456	11.62	0.0971	30	107.463	10.35	0.1299	30
26.939	11.6	0.0976	30	108.892	10.33	0.1305	30
28.367	11.58	0.0982	30	110.375	10.3	0.1312	30
29.85	11.55	0.0987	30	111.803	10.28	0.1318	30
31.333	11.53	0.0993	30	113.231	10.26	0.1324	30
32.816	11.51	0.0998	30	114.714	10.24	0.1331	30
34.299	11.49	0.1005	30	116.143	10.21	0.1336	30
35.782	11.46	0.1011	30	117.625	10.19	0.1343	30
37.265	11.44	0.1016	30	119.081	10.17	0.1349	30
38.749	11.42	0.1022	30	120.564	10.14	0.1355	30
40.177	11.39	0.1027	30	121.992	10.12	0.1362	30
41.605	11.37	0.1032	30	123.475	10.1	0.1368	30
43.088	11.35	0.1038	30	124.958	10.08	0.1375	30
44.517	11.33	0.1044	30	126.469	10.05	0.1382	30
46	11.3	0.1049	30	127.952	10.03	0.1388	30
47.427	11.28	0.1054	30	129.435	10.01	0.1394	30
48.91	11.26	0.1061	30	130.945	9.979	0.1401	30
50.366	11.24	0.1067	30	132.428	9.957	0.1408	30
51.849	11.21	0.1072	30	133.856	9.934	0.1414	30
53.277	11.19	0.1077	30	135.34	9.911	0.1421	30
54.76	11.17	0.1083	30	136.768	9.889	0.1427	30
56.188	11.15	0.1089	30	138.251	9.866	0.1433	30
57.616	11.12	0.1095	30	139.679	9.844	0.1441	30

59.099	11.1	0.1101	30
60.527	11.08	0.1106	30
62.011	11.06	0.1111	30
63.439	11.03	0.1117	30
64.922	11.01	0.1123	30
66.405	10.99	0.1128	30
67.888	10.96	0.1134	30
69.398	10.94	0.1141	30
70.881	10.92	0.1147	30
72.365	10.89	0.1153	30
73.848	10.87	0.1159	30
75.275	10.85	0.1165	30
76.758	10.83	0.1171	30
78.186	10.8	0.1177	30
79.669	10.78	0.1183	30
81.097	10.76	0.1188	30
164.534	9.457	0.1556	30
166.017	9.434	0.1564	30
167.5	9.411	0.1571	30
168.928	9.389	0.1578	30
170.411	9.366	0.1585	30
171.838	9.344	0.1592	30
173.321	9.321	0.1601	30
174.749	9.298	0.1607	30
176.232	9.275	0.1614	30
177.66	9.253	0.1621	30
179.143	9.23	0.1627	30
180.599	9.207	0.1635	30
182.082	9.185	0.1642	30
183.51	9.163	0.1649	30
184.938	9.14	0.1657	30
186.421	9.117	0.1664	30
187.85	9.095	0.1671	30
189.333	9.072	0.1677	30
190.76	9.05	0.1684	30
192.243	9.027	0.1691	30
193.671	9.004	0.1699	30
195.154	8.981	0.1706	30
196.637	8.958	0.1714	30
198.12	8.935	0.1721	30
199.603	8.912	0.1729	30
201.086	8.889	0.1736	30
202.569	8.866	0.1743	30
204.052	8.843	0.1751	30
205.48	8.82	0.1758	30
206.963	8.798	0.1766	30
208.392	8.775	0.1774	30

141.107	9.821	0.1447	30
142.59	9.798	0.1454	30
144.019	9.776	0.1461	30
145.501	9.753	0.1467	30
146.929	9.731	0.1474	30
148.412	9.708	0.1481	30
149.868	9.685	0.1487	30
151.351	9.663	0.1494	30
152.779	9.64	0.1501	30
154.207	9.618	0.1507	30
155.69	9.595	0.1515	30
157.118	9.572	0.1522	30
158.602	9.549	0.1528	30
160.084	9.526	0.1534	30
161.567	9.503	0.1542	30
163.051	9.48	0.1548	30
246.455	8.185	0.1979	30
247.938	8.162	0.1988	30
249.366	8.139	0.1995	30
250.849	8.116	0.2004	30
252.277	8.094	0.2012	30
253.76	8.071	0.2021	30
255.243	8.048	0.2027	30
256.726	8.025	0.2035	30
258.209	8.002	0.2044	30
259.692	7.979	0.2053	30
261.175	7.956	0.2061	30
262.658	7.933	0.2071	30
264.086	7.91	0.2077	30
265.514	7.888	0.2086	30
266.997	7.865	0.2095	30
268.425	7.843	0.2102	30
269.908	7.82	0.2111	30
271.335	7.798	0.2121	30
272.846	7.774	0.2129	30
274.274	7.752	0.2137	30
275.757	7.729	0.2145	30
277.185	7.707	0.2154	30
278.668	7.684	0.2163	30
280.097	7.662	0.2171	30
281.525	7.639	0.2181	30
283.008	7.616	0.2188	30
284.437	7.594	0.2197	30
285.919	7.571	0.2206	30
287.348	7.549	0.2215	30
288.831	7.525	0.2224	30
290.313	7.502	0.2232	30

209.82	8.753	0.1782	30
211.331	8.73	0.1791	30
212.759	8.708	0.1799	30
214.242	8.685	0.1805	30
215.67	8.662	0.1813	30
217.153	8.639	0.1821	30
218.581	8.617	0.1828	30
220.063	8.594	0.1835	30
221.492	8.572	0.1843	30
222.975	8.549	0.1851	30
224.403	8.527	0.1858	30
225.831	8.504	0.1867	30
227.314	8.481	0.1874	30
228.77	8.459	0.1882	30
230.28	8.435	0.1891	30
231.763	8.413	0.1898	30
233.246	8.39	0.1906	30
234.729	8.367	0.1913	30
236.212	8.344	0.1922	30
237.695	8.321	0.1931	30
239.178	8.298	0.1938	30
240.606	8.275	0.1946	30
242.117	8.252	0.1954	30
243.544	8.23	0.1961	30
245.027	8.207	0.1971	30
328.377	6.911	0.2475	30
329.86	6.888	0.2485	30
331.371	6.865	0.2495	30
332.854	6.842	0.2506	30
334.364	6.818	0.2516	30
335.792	6.797	0.2524	30
337.22	6.774	0.2534	30
338.703	6.751	0.2544	30
340.131	6.729	0.2554	30
341.642	6.706	0.2564	30
343.069	6.684	0.2573	30
344.552	6.661	0.2584	30
345.98	6.639	0.2594	30
347.463	6.615	0.2603	30
348.892	6.593	0.2612	30
350.375	6.57	0.2623	30
351.803	6.548	0.2635	30
353.231	6.526	0.2645	30
354.715	6.503	0.2654	30
356.143	6.48	0.2664	30
357.626	6.457	0.2675	30
359.054	6.435	0.2685	30

291.824	7.479	0.2242	30
293.307	7.456	0.2251	30
294.79	7.433	0.2261	30
296.273	7.41	0.2271	30
297.756	7.387	0.2278	30
299.184	7.365	0.2287	30
300.667	7.342	0.2296	30
302.095	7.32	0.2304	30
303.578	7.297	0.2314	30
305.006	7.274	0.2323	30
306.489	7.251	0.2332	30
307.917	7.229	0.2342	30
309.346	7.207	0.2352	30
310.856	7.184	0.2362	30
312.284	7.162	0.2371	30
313.767	7.139	0.2381	30
315.195	7.116	0.2389	30
316.678	7.093	0.2399	30
318.105	7.071	0.2408	30
319.588	7.048	0.2417	30
321.017	7.025	0.2428	30
322.5	7.003	0.2438	30
323.928	6.98	0.2447	30
325.411	6.957	0.2456	30
326.894	6.934	0.2465	30
574.281	3.091	0.4759	30
575.737	3.068	0.4779	30
577.165	3.046	0.4801	30
578.648	3.023	0.4821	30
580.131	3	0.4841	30
581.614	2.978	0.4861	30
583.042	2.955	0.4881	30
584.524	2.932	0.4902	30
585.953	2.91	0.4923	30
587.436	2.887	0.4944	30
588.864	2.865	0.4966	30
590.292	2.843	0.4987	30
591.775	2.82	0.5011	30
593.203	2.797	0.5033	30
594.714	2.774	0.5055	30
596.142	2.752	0.5077	30
597.625	2.729	0.5099	30
599.108	2.706	0.5122	30
600.591	2.683	0.5146	30
602.074	2.66	0.5171	30
603.557	2.637	0.5192	30
605.041	2.614	0.5217	30

360.564	6.411	0.2696	30
362.047	6.389	0.2705	30
363.53	6.366	0.2715	30
365.013	6.343	0.2726	30
366.496	6.32	0.2738	30
367.979	6.297	0.2749	30
369.462	6.274	0.2759	30
370.89	6.251	0.2771	30
372.4	6.228	0.2781	30
373.828	6.206	0.2792	30
375.312	6.183	0.2802	30
376.74	6.161	0.2813	30
378.223	6.138	0.2824	30
379.651	6.115	0.2835	30
381.079	6.093	0.2846	30
382.562	6.07	0.2858	30
384.073	6.047	0.2869	30
385.556	6.024	0.2881	30
387.039	6.001	0.2891	30
388.521	5.978	0.2901	30
390.005	5.955	0.2913	30
391.488	5.932	0.2925	30
392.916	5.909	0.2936	30
394.398	5.886	0.2948	30
395.826	5.864	0.2959	30
397.309	5.841	0.2971	30
398.737	5.819	0.2981	30
400.22	5.796	0.2993	30
401.648	5.774	0.3004	30
403.159	5.75	0.3015	30
404.587	5.728	0.3026	30
406.07	5.705	0.3037	30
407.498	5.683	0.3049	30
408.926	5.661	0.3061	30
410.409	5.638	0.3073	30
411:837	5.615	0.3085	30
413.32	5.592	0.3095	30
414.748	5.57	0.3107	30
416.23	5.547	0.3121	30
417.659	5.525	0.3131	30
419.142	5.502	0.3142	30
420.57	5.48	0.3154	30
422.025	5.457	0.3166	30
423.508	5.434	0.3178	30
424.937	5.412	0.3189	30
426.419	5.389	0.3201	30
427.848	5.367	0.3214	30

606.551	2.59	0.5241	30
607.979	2.568	0.5264	30
609.461	2.545	0.5289	30
610.889	2.523	0.5313	30
612.372	2.5	0.5338	30
613.8	2.478	0.5362	30
615.284	2.455	0.5389	30
616.712	2.432	0.5414	30
618.14	2.41	0.5439	30
619.624	2.387	0.5465	30
621.134	2.364	0.5492	30
622.617	2.341	0.5519	30
624.1	2.318	0.5547	30
625.583	2.295	0.5575	30
627.066	2.272	0.5603	30
628.549	2.249	0.5631	30
630.032	2.226	0.5661	30
631.459	2.203	0.5691	30
632.887	2.181	0.5718	30
634.37	2.158	0.5748	30
635.798	2.136	0.5774	30
637.308	2.112	0.5803	30
638.736	2.091	0.5832	30
640.219	2.068	0.5863	30
641.647	2.045	0.5893	30
643.131	2.022	0.5925	30
644.559	2	0.5957	30
645.987	1.978	0.5991	30
647.471	1.955	0.6023	30
648.899	1.932	0.6055	30
650.382	1.909	0.6091	30
651.865	1.886	0.6123	30
653.293	1.864	0.6157	30
654.721	1.842	0.6194	30
487.909	4.433	0.3765	30
489.337	4.411	0.3781	30
490.82	4.388	0.3795	30
492.303	4.365	0.3811	30
493.786	4.342	0.3825	30
495.269	4.319	0.3838	30
496.752	4.296	0.3854	30
498.235	4.273	0.3869	30
499.718	4.25	0.3885	30
501.146	4.227	0.3899	30
502.629	4.204	0.3913	30
504.058	4.182	0.3929	30
505.486	4.16	0.3944	30

429.331	5.344	0.3226	30
430.758	5.321	0.3239	30
432.241	5.298	0.3251	30
433.724	5.275	0.3265	30
435.207	5.252	0.3277	30
436.69	5.229	0.3291	30
438.173	5.206	0.3304	30
439.656	5.183	0.3317	30
441.139	5.16	0.3331	30
442.567	5.138	0.3342	30
444.05	5.115	0.3355	30
445.478	5.092	0.3368	30
446.961	5.069	0.3381	30
448.39	5.047	0.3394	30
449.818	5.025	0.3407	30
451.301	5.002	0.3419	30
452.757	4.979	0.3432	30
454.24	4.956	0.3444	30
455.723	4.933	0.3458	30
457.206	4.91	0.3471	30
458.688	4.887	0.3485	30
460.171	4.864	0.3499	30
461.655	4.841	0.3513	30
463.138	4.818	0.3527	30
464.593	4.795	0.3541	30
466.076	4.773	0.3553	30
467.504	4.75	0.3566	30
468.987	4.727	0.3581	30
470.415	4.705	0.3594	30
471.898	4.682	0.3607	30
473.326	4.66	0.3621	30
474.809	4.637	0.3635	30
476.237	4.615	0.3651	30
477.666	4.592	0.3665	30
479.148	4.569	0.3678	30
480.577	4.547	0.3692	30
482.06	4.524	0.3707	30
483.515	4.501	0.3722	30
484.998	4.479	0.3735	30
486.426	4.456	0.3751	30
565.438	3.228	0.4642	30
566.921	3.205	0.4663	30
568.404	3.182	0.4682	30
656.231	1.818	0.623	30
657.714	1.796	0.6265	30
659.197	1.772	0.6303	30
660.708	1.749	0.634	30
662.191	1.726	0.6379	30

506.969	4.137	0.3961	30
508.452	4.114	0.3974	30
509.88	4.091	0.3991	30
511.308	4.069	0.4005	30
512.791	4.046	0.4022	30
514.246	4.024	0.4036	30
515.729	4.001	0.4051	30
517.157	3.979	0.4067	30
518.641	3.956	0.4084	30
520.069	3.933	0.4101	30
521.497	3.911	0.4116	30
522.98	3.888	0.4133	30
524.409	3.865	0.4149	30
525.892	3.842	0.4166	30
527.375	3.819	0.4183	30
528.858	3.796	0.4201	30
530.341	3.773	0.4216	30
531.824	3.75	0.4235	30
533.307	3.727	0.4251	30
534.79	3.704	0.4269	30
536.218	3.682	0.4285	30
537.701	3.659	0.4302	30
539.128	3.637	0.4318	30
540.611	3.614	0.4335	30
542.04	3.591	0.4354	30
543.522	3.568	0.4371	30
544.978	3.546	0.4387	30
546.461	3.523	0.4405	30
547.889	3.501	0.4422	30
549.317	3.479	0.4441	30
550.8	3.456	0.4456	30
552.229	3.433	0.4475	30
553.711	3.41	0.4493	30
555.139	3.388	0.4511	30
556.622	3.365	0.4529	30
558.05	3.343	0.4547	30
559.533	3.32	0.4565	30
560.961	3.297	0.4584	30
562.444	3.274	0.4604	30
563.955	3.251	0.4626	30
569.887	3.159	0.4702	30
571.37	3.136	0.4721	30
572.798	3.114	0.4741	30
729.422	0.6813	0.937	30
730.905	0.6583	0.9491	30
732.388	0.6353	0.9615	30
733.871	0.6123	0.9746	30
735.354	0.5892	0.9879	30

663.674	1.703	0.6416	30
665.157	1.68	0.6455	30
666.585	1.658	0.6493	30
668.096	1.635	0.6536	30
669.524	1.613	0.658	30
671.007	1.59	0.6621	30
672.435	1.568	0.6663	30
673.863	1.545	0.6706	30
675.346	1.522	0.675	30
676.774	1.5	0.6794	30
678.257	1.477	0.684	30
679.685	1.455	0.6886	30
681.168	1.432	0.6932	30
682.596	1.409	0.6982	30
684.079	1.386	0.7034	30
685.507	1.364	0.7082	30
687.018	1.341	0.7136	30
688.446	1.319	0.7186	30
689.875	1.296	0.7239	30
691.358	1.273	0.7294	30
692.841	1.25	0.7352	30
694.324	1.227	0.7409	30
695.807	1.204	0.7469	30
697.29	1.181	0.7532	30
698.773	1.158	0.7592	30
700.256	1.135	0.7658	30
701.684	1.113	0.7721	30
703.167	1.09	0.7787	30
704.595	1.067	0.7857	30
706.105	1.044	0.7929	30
707.533	1.022	0.7997	30
709.016	0.9987	0.8072	30
710.444	0.9764	0.8145	30
711.927	0.9534	0.8224	30
713.355	0.9311	0.8302	30
714.839	0.9081	0.8384	30
716.267	0.8858	0.8469	30
717.695	0.8635	0.8554	30
719.178	0.8405	0.8648	30
720.606	0.8182	0.8738	30
722.089	0.7952	0.8834	30
723.517	0.7729	0.893	30
725.028	0.7496	0.9037	30
726.456	0.7274	0.914	30
727.938	0.7044	0.9254	30

736.864	0.5655	1.0026	30
738.292	0.5439	1.0165	30
739.775	0.5209	1.0319	30
741.204	0.4986	1.0476	30
742.687	0.4756	1.0646	30
744.115	0.4533	1.0817	30
745.598	0.4301	1.1002	30
747.025	0.408	1.119	30
748.454	0.3858	1.1386	30
749.937	0.3625	1.1602	30
751.447	0.3394	1.1833	30
752.93	0.3164	1.2072	30
754.413	0.2934	1.233	30
755.923	0.27	1.2612	30
757.406	0.2474	1.2906	30
758.889	0.2242	1.3223	30
760.316	0.2021	1.3555	30
761.799	0.179	1.3931	30
763.228	0.1566	1.4332	30
764.71	0.1337	1.4779	30
766.139	0.1115	1.527	30
767.622	0.0884	1.5836	30
769.05	0.0661	1.647	30
770.533	0.0432	1.7193	30
771.96	0.0209	1.7876	30
773.443	0	1.8372	30

Appendix B

Table 2. The calculated critical current density, pinning force, reduced force, and reduced magnetic field for 2.5% Al At T= 77 K.

M1	M2	H	ΔM	J_c	F	H/H_{max}	F/F_{max}
8.60E-05	-2.95E-05	200	1.16E-04	6.93E-03	1.39E+0	0.038677	3.54E-01
9.90E-05	-9.16E-06	405	1.08E-04	6.49E-03	2.63E+0	0.078321	6.72E-01
1.05E-04	1.40E-05	604	9.10E-05	5.46E-03	3.30E+0	0.116805	8.43E-01
1.12E-04	3.40E-05	801	7.80E-05	4.68E-03	3.75E+0	0.154902	9.59E-01
1.17E-04	5.19E-05	1000	6.51E-05	3.91E-03	3.91E+0	0.193386	9.99E-01
1.21E-04	6.96E-05	1201	5.14E-05	3.08E-03	3.70E+0	0.232257	9.47E-01
1.24E-04	7.99E-05	1400	4.41E-05	2.65E-03	3.70E+0	0.270741	9.47E-01
1.27E-04	8.87E-05	1602	3.83E-05	2.30E-03	3.68E+0	0.309805	9.42E-01
1.29E-04	9.50E-05	1800	3.40E-05	2.04E-03	3.67E+0	0.348095	9.39E-01
1.29E-04	1.04E-04	2000	2.50E-05	1.50E-03	3.00E+0	0.386772	7.67E-01
1.31E-04	1.08E-04	2200	2.30E-05	1.38E-03	3.04E+0	0.42545	7.76E-01
1.28E-04	1.10E-04	2400	1.80E-05	1.08E-03	2.59E+0	0.464127	6.63E-01
1.27E-04	1.12E-04	2602	1.50E-05	9.00E-04	2.34E+0	0.503191	5.99E-01
1.27E-04	1.15E-04	2800	1.20E-05	7.20E-04	2.02E+0	0.541481	5.16E-01
1.26E-04	1.13E-04	3000	1.30E-05	7.80E-04	2.34E+0	0.580159	5.98E-01
1.23E-04	1.13E-04	3202	1.00E-05	6.00E-04	1.92E+0	0.619223	4.91E-01
1.22E-04	1.14E-04	3400	8.00E-06	4.80E-04	1.63E+0	0.657513	4.17E-01
1.23E-04	1.14E-04	3602	9.00E-06	5.40E-04	1.95E+0	0.696577	4.97E-01
1.21E-04	1.12E-04	3801	9.00E-06	5.40E-04	2.05E+0	0.735061	5.25E-01
1.18E-04	1.12E-04	4000	6.00E-06	3.60E-04	1.44E+0	0.773545	3.68E-01
1.18E-04	1.12E-04	4202	6.00E-06	3.60E-04	1.51E+0	0.812609	3.87E-01
1.14E-04	1.08E-04	4402	6.00E-06	3.60E-04	1.58E+0	0.851286	4.05E-01
1.13E-04	1.08E-04	4601	5.00E-06	3.00E-04	1.38E+0	0.88977	3.53E-01
1.10E-04	1.07E-04	4800	3.00E-06	1.80E-04	8.64E-0	0.928254	2.21E-01
1.08E-04	1.01E-04	5000	7.00E-06	4.20E-04	2.10E+0	0.966931	5.37E-01
1.05E-04	1.01E-04	5171	4.00E-06	2.40E-04	1.24E+0	1	3.17E-01

Where M_1 is the magnetization while increasing the applied magnetic field

M_2 is the magnetization while decreasing the applied magnetic field

J_c is the critical current density

H is the applied magntic field

F is the pinning force

Appendix C

Table 3. The parameters and concentrations of Al-doped YBCO superconducting thin films used in this study as provided from the source.

Al concentration %	Sample parameters	Tc (K)
0	4.9×5.1 mm^2	90
1	5×5.1 mm^2	89
1.5	5 ×5 mm^2	86
2	4.9×5 mm^2	82
2.5	5×5 mm^2	78
5	4.5×5.1 mm^2	26

الخلاصة

لقـد تـم إستخدام البيانات الممغنطة لشرائح YBCO الفائقة الإيصالية والمعجونة بالألمنيوم والمحضرة باستخدام الليزر لإيجاد قيم التيار الحرج ودرجة الحرارة الحرجة ودراسة القابلية المغناطيسـة (المغـنطة) لعيـنات متفاوتة في درجة تركيز الألمنيوم (0-2.5%). وبينت الدراسـة أن النـتائج تعـتمد بشكل كبير على تركيز العجينة في الشرائح ، ولم يرصد أي اخـتلاف في منحيات المغنطة التي كانت متماثلة في السلوك بشكل عام وكذلك الحال بالنسبة لمنحنيات التخلف المغناطيسي.

كما تم استخدام منحنيات حلقات المغنطة لحساب كثافة التيار الحرج(J_c)، ووجد أن نتائج التيار الحرج تتفق مع القانون التالي

$$J_c = J_0(T)(1-T/T_c)^n \qquad \text{with } n \approx 2.3$$

حيـث n تمـثل المعـامل الأسـي الذي قيمته المثالية تعادل 2.42 . كما تم دراسة القوة المسـمارية عـند درجة حرارة مختلفة للعينات المعطاة، وتبين أن هذه القوة يمكن أن تمثل بالقانون التالي

$$F_h = F_{p0}(T)\,h^p(1-h)^q$$

حيث h المجال المنخفض و p و q هي المعاملات الأسية والتي تتراوح قيمها ما بين 0.70± 0.02 إلـى 1.72±0.05 ، علـى الترتيب. لقد وجد أن القوة المسمارية تتمتع بقيمة عظمى عند دراسة منحنيات القوة المسمارية مع القيم العظمى للمجال المغناطيسي، أي علاقة F مع H_{max}. وبشكل عام يمكن كتابة هذه العلاقة على شكل إقتران أسي يعطى بالعلاقة التالية

$$F_p \propto H_{max}^{n}$$

كمـــا بينت الدراسة إن مجمل القوانين التي تمثل سلوك التيار الحرج والدرجة الحرجة والقوة المســـمارية تتفق مع نموذج التدفق الخطي المجزىء (FLS) عند درجات الحرارة المنخفضة كما أنها تتفق مع النموذج عند درجات الحرارة حول الدرجة الحرجة.